Assessment of New 2- and 3-FP Plasma and Coil Configurations

Long-Poe Ku
Princeton Plasma Physics Laboratory

ARIES Project Meeting, June 14-15, 2005
University of Wisconsin, Madison WI

Topics of Discussion

- New coils for A~2.5, two field-period configurations
  - MHH2-1104, coil properties and characteristics of free-boundary plasma equilibria
  - MHH2-K14, coil properties and characteristics of free-boundary plasma equilibria
- Development of A~6.0, three field-period configurations
  - KJC167, physics characteristics and new coil design
- Summary and Plans

MHH2 -- 1104 and K14

MHH2-1104 and MHH2–K14 are two-field period, aspect ratio ~2.65 configurations introduced in the last project meeting. These configurations have low field ripples, resulting in excellent confinement for α particles.

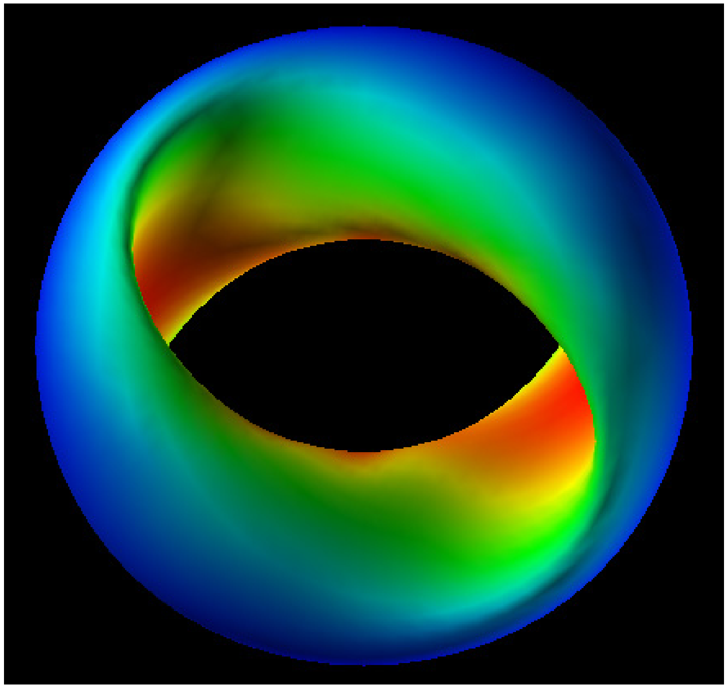

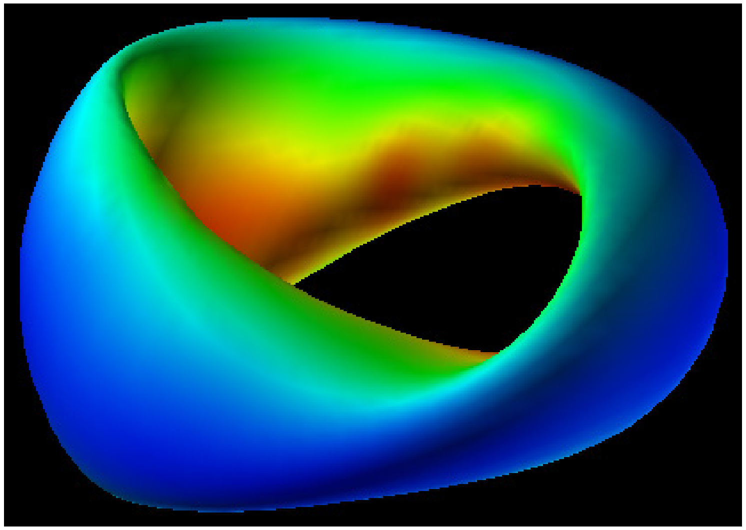

Plane and perspective views of the last LCMS geometry and |B| in real space.

The two configurations differ in the profile of the total rotational transform.

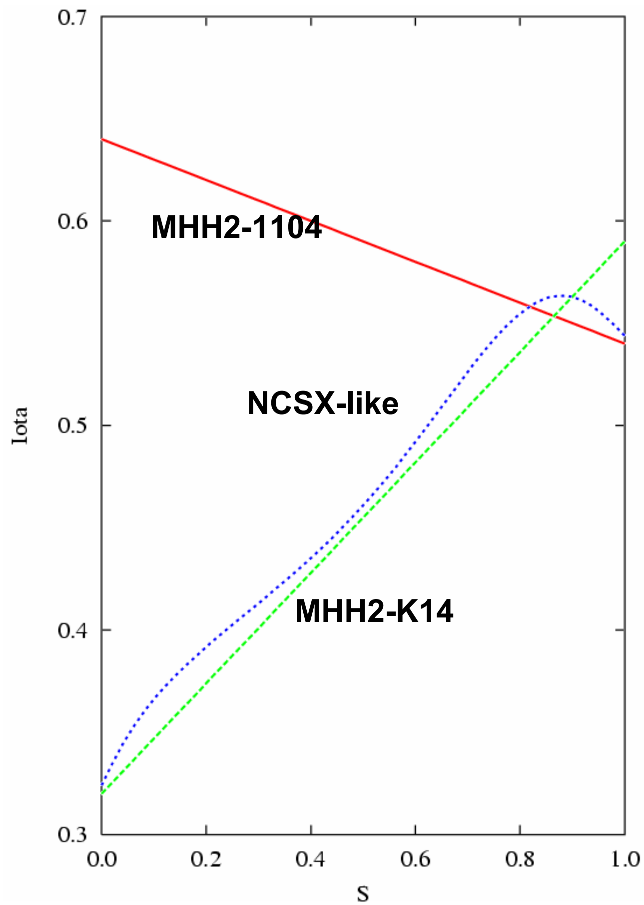

Rotational transform versus normalized toroidal flux. Ip/R-B ~0.21 MA/m-T

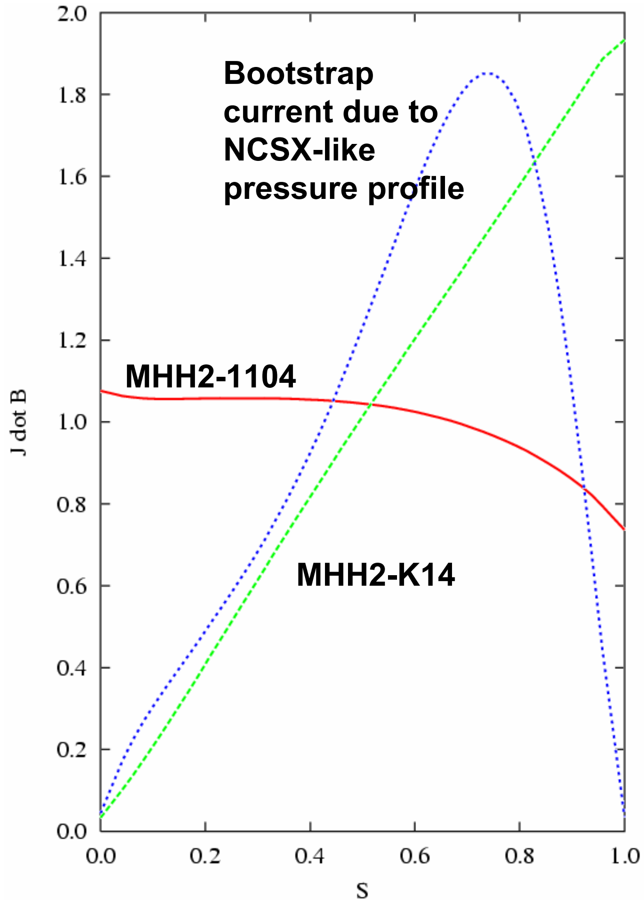

Normalized toroidal current density versus normalized toroidal flux for the iota profiles shown on the left.

- **Initial designs of MHH2 coils discussed in the last meeting were obtained by solving current potentials on a prescribed winding surface.**
  - **Despite small residues of the normal fields on the LCMS, the designs failed to provide some important physics properties that are the basis of developing the original configurations, such as the confinement of α particles, in the free-boundary equilibria.**
  - **The designs also had some poor engineering properties, such as the small separation distances between coils in some locations, resulting in large B_{max}/B_0.**

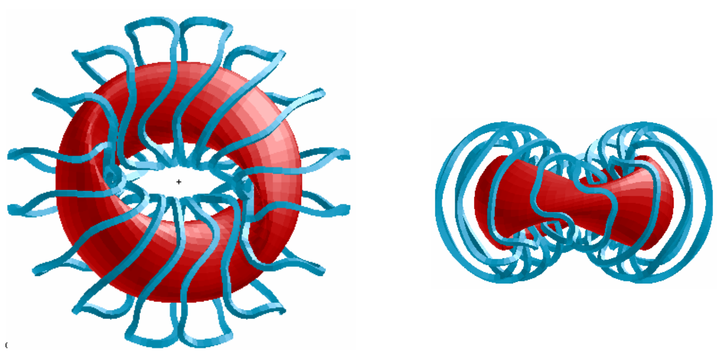

MHH2-1104

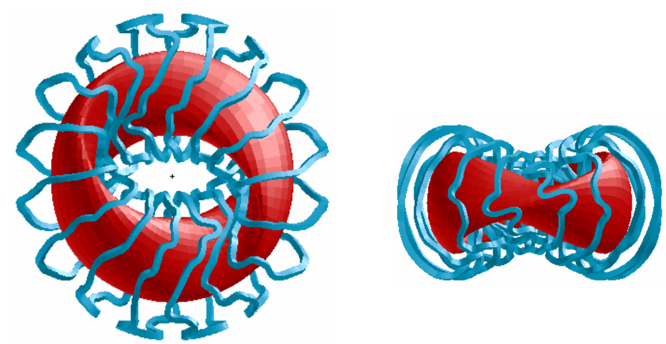

MHH2-K14_V

- **More rigorous design optimizations now lead to new designs of coils with significantly improved engineering properties and physics performance.**
  - **Using free-boundary equilibria to target physics in optimization**
    - **Minimize QA residues, effective ripples and collisionless α loss, but not necessarily reproduce the original fixed-boundary configuration.**
    - **Constrain rotational transform or current density at 5% β.**
    - **Constrain R-B_{tor} or aspect ratio.**
  - **Coil geometry, winding surface and coil currents allow to vary to target engineering properties**
    - **Constrain coil-coil separation, coil-plasma separation, radius of curvature.**

We have demonstrated that low α loss may be achieved with discrete coils in MHH2 at a finite β and that these coils have the properties essential to designing a compact reactor!

We shall discuss three sets of coil designs, all for plasmas at 5% β --

- **Comparison of coil geometry, coil complexity and properties of free-boundary equilibria for MHH2-1104 and MHH2-K14.**
  - **Coils are similar for similar constraints.**
  - **Further improvement in physics possible with free-boundary equilibria.**

- **A coil design for MHH2-K14 that has very low α loss.**
  - **Optimized by prescribing a total rotational transform.**
  - **Superior QA comes at the expense of reduced external rotational transform.**

- **A coil design for rotational transforms more consistent with the bootstrap current.**
  - **Optimized by prescribing a plasma current density profile while constraining the total rotational transform.**
  - **Equilibrium has good QA and low α loss.**

Comparison of coils for MHH2-1104 and MHH2-K14

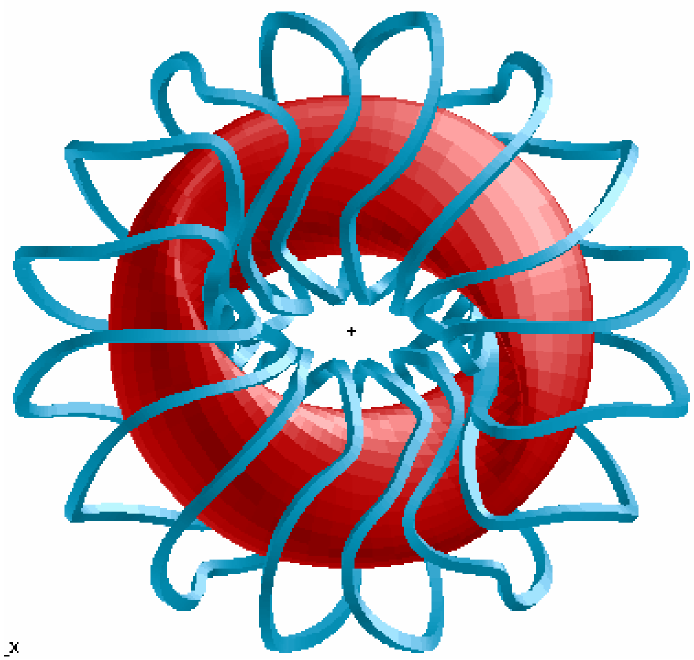

Modular Coils for MHH2-1104: 1104ACS

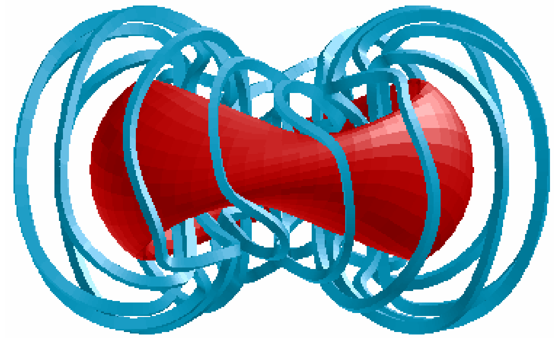

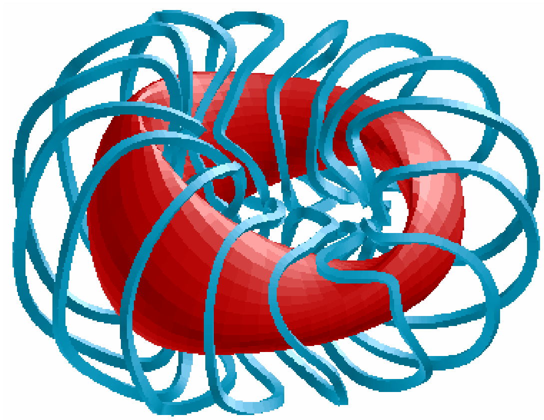

No. of Coils: 8/period

Different Types of Coils: 4

R/Δ_{min} (coil-plasma)=5.3

R/Δ_{min} (coil-coil)=12.5

I /R-B (max)=0.32 MA/m-T

B(max)/B(0) = 2.2 for 0.4 m x 0.4 m conductor

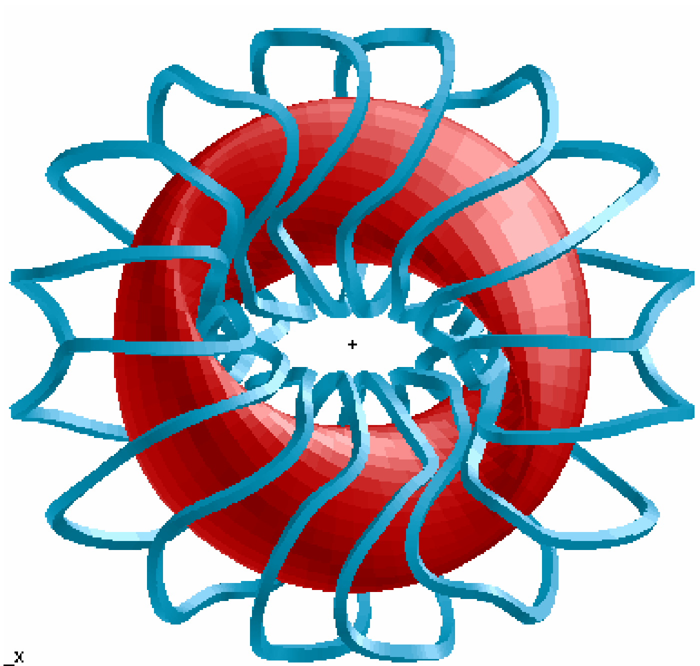

Modular Coils for MHH2-K14: K14GH

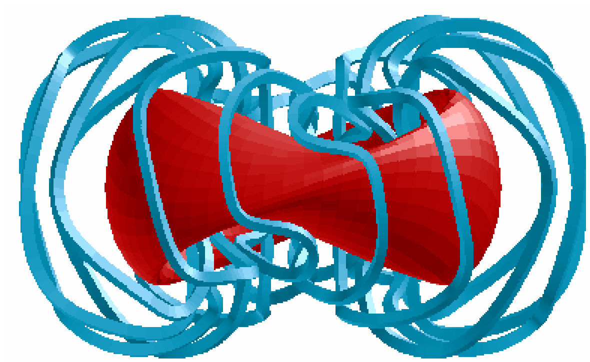

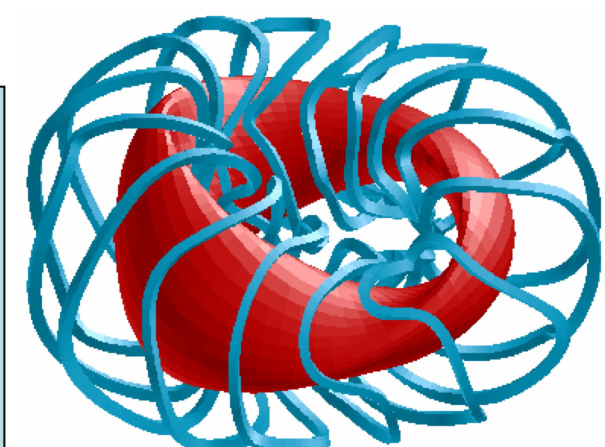

No. of Coils: 8/period

Different Types of Coils: 4

R/Δ_{min} (coil-plasma)=5.4

R/Δ_{min} (coil-coil)=12.2

I /R-B (max)=0.32 MA/m-T

B(max)/B(0) = 2.0 for 0.4 m x 0.4 m conductor

Coil winding surface and coil contours viewed on the U-V plane – 1104ACS.

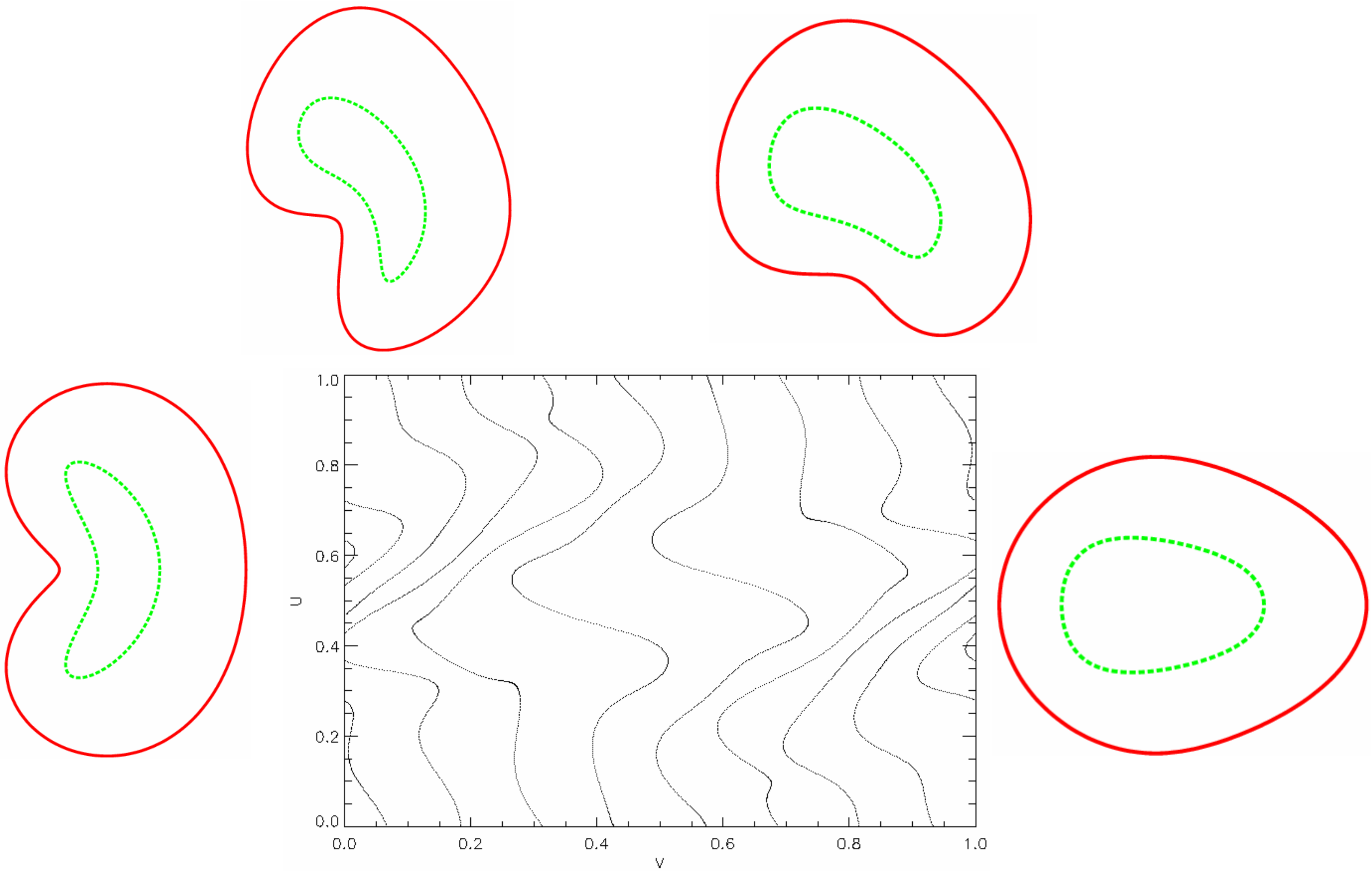

Coil winding surface and coil contours viewed on the U-V plane – K14GH

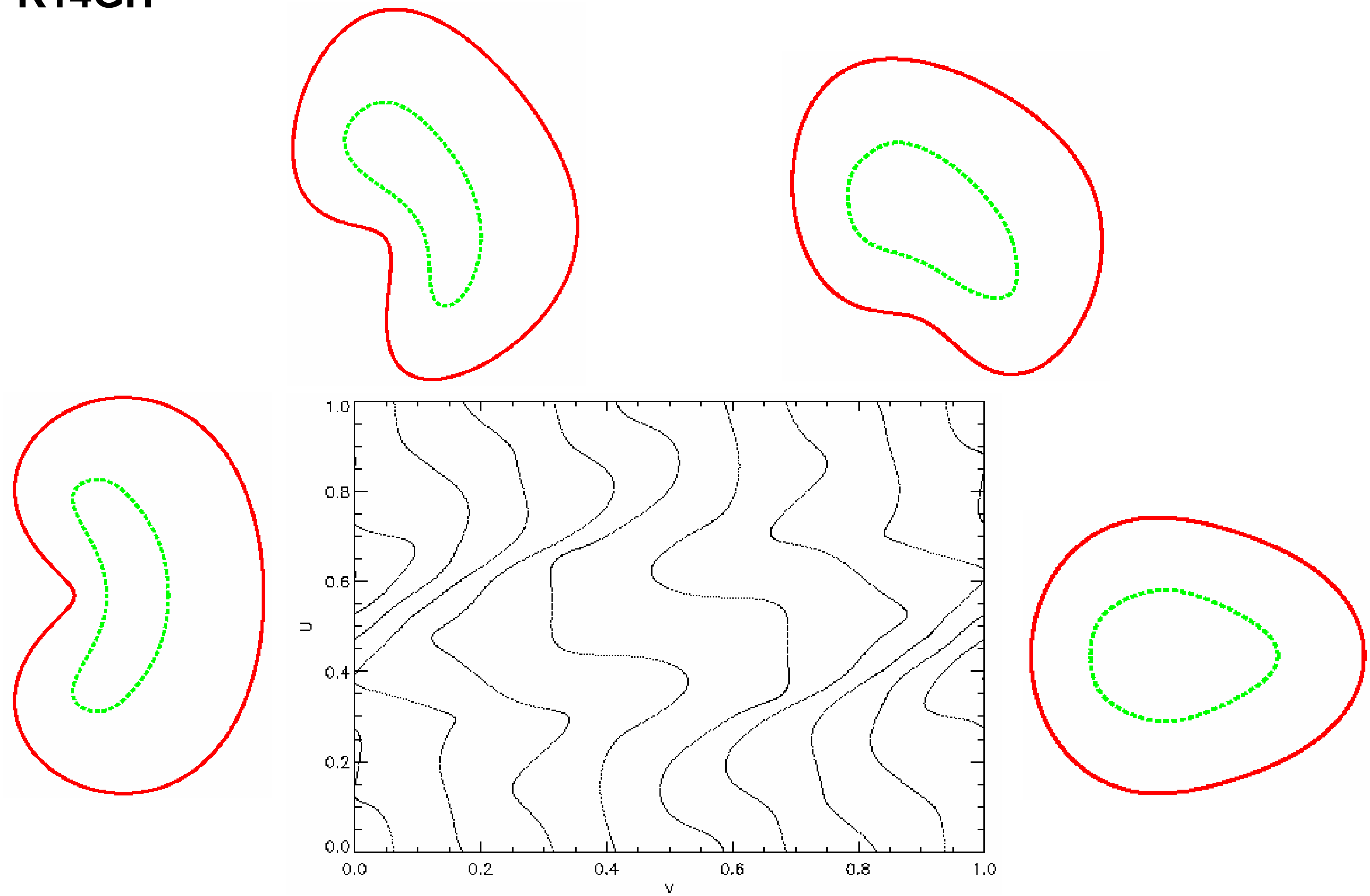

Comparison of surface shapes of fixed and free-boundary equilibria having the same amount of enclosed toroidal flux.

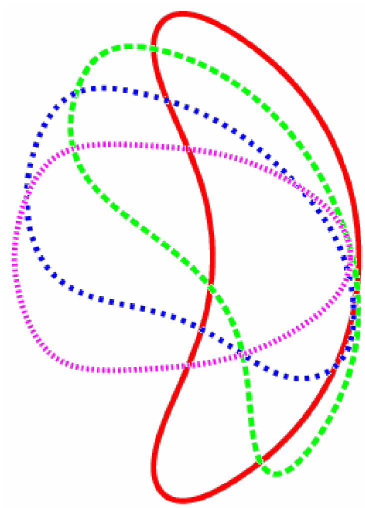

1104 and 1104ACS

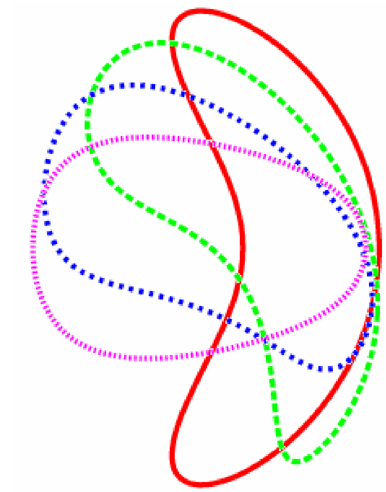

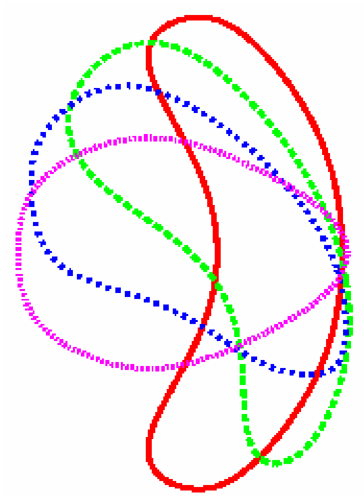

K14 and K14GH

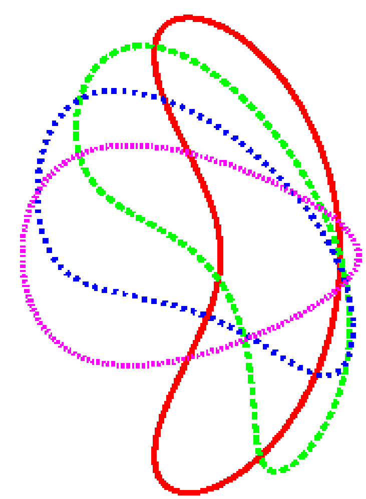

LCMS of the free-boundary equilibria constructed from coils using VMEC.

LCMS of the original fixed-boundary plasma.

Comparison of residues in magnetic spectrum, reconstructed with 1104ACS versus the original, showing that the free-boundary equilibrium has excellent QA properties.

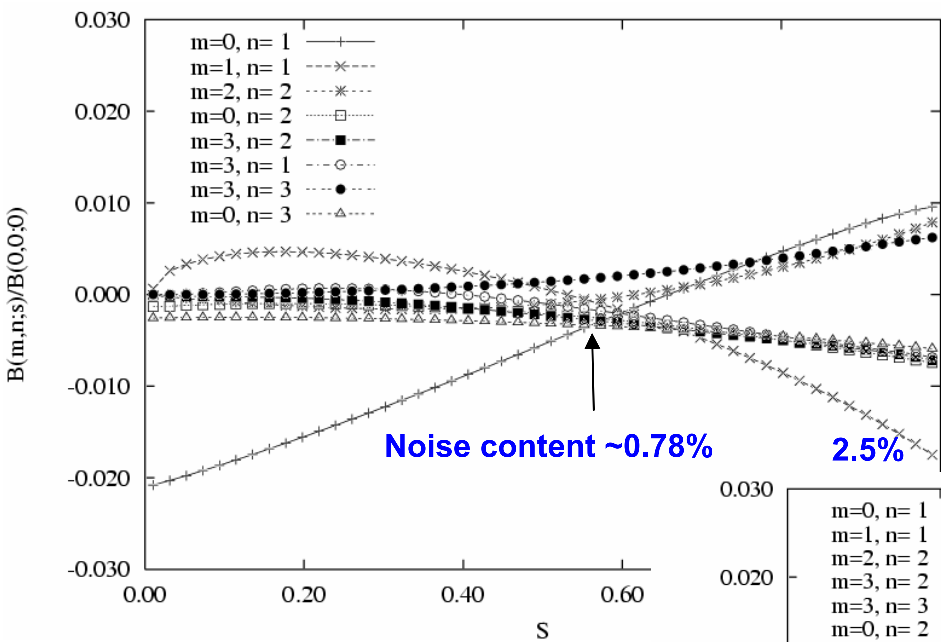

Free–boundary plasma, 1104ACS coils:

Effective ripple <0.53%

α energy loss in model calculation ~5%

Fixed –boundary plasma:

Effective ripple <0.35%

α energy loss in model calculation ~2%

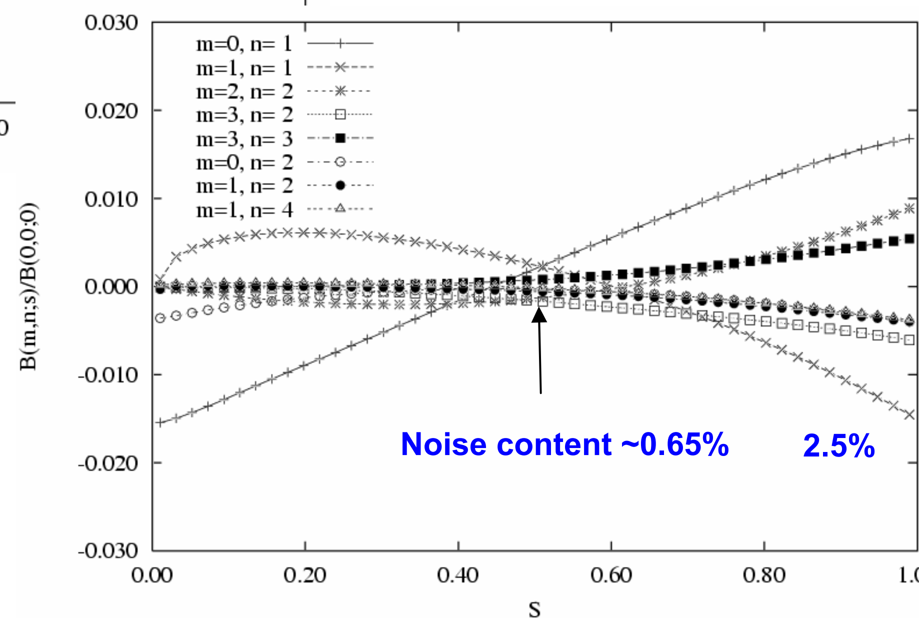

Comparison of residues in magnetic spectrum, reconstructed with K14GH versus the original, showing that the free-boundary equilibrium has lower residues and comparable ε_{eff} and α energy loss.

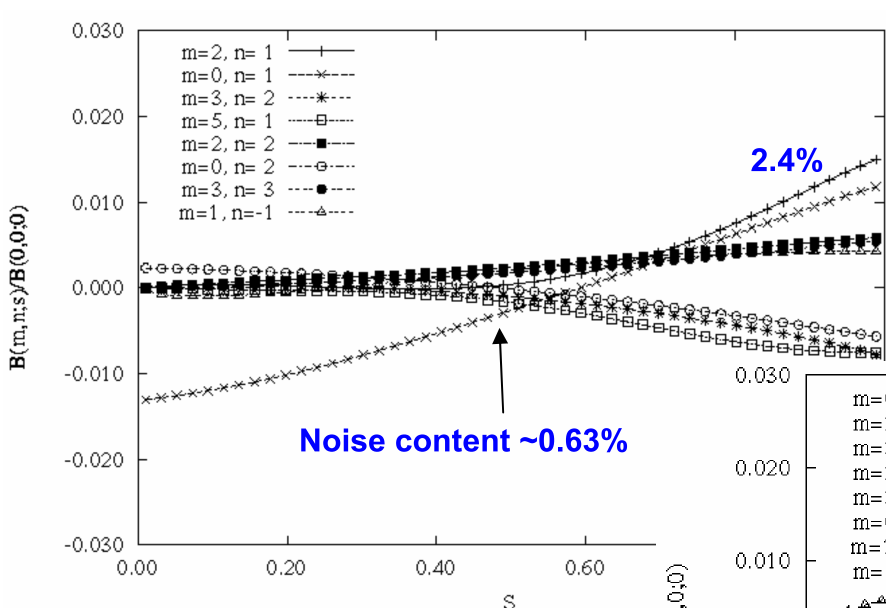

Free–boundary plasma, K14GH coils:

Effective ripple <0.92%

α energy loss in model calculation ~8.5%

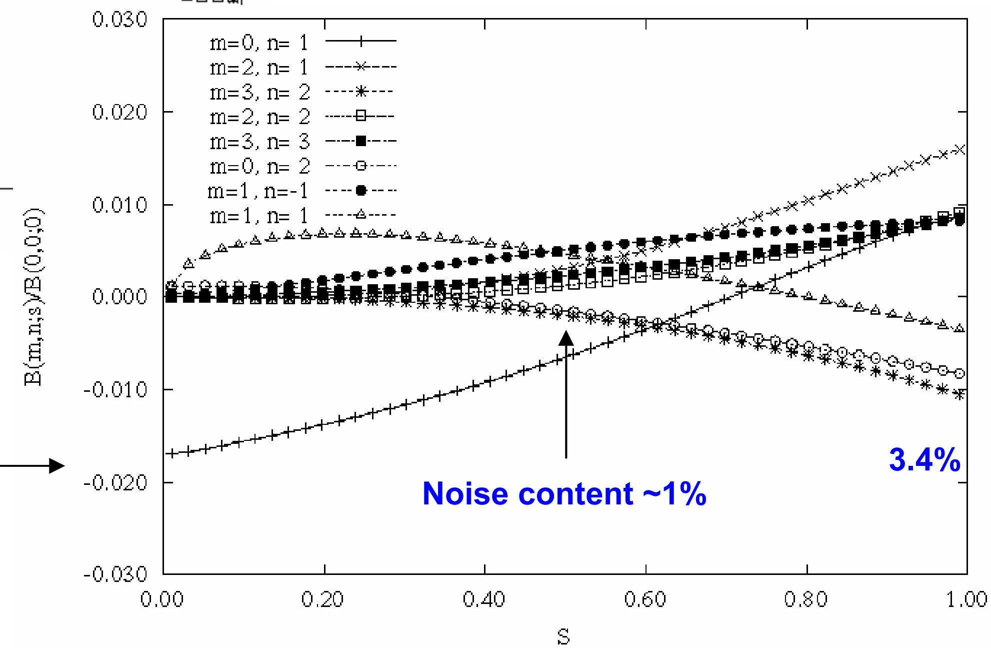

Fixed –boundary plasma:

Effective ripple <0.78%

α energy loss in model calculation ~6.5%

Optimizations for the above coils were carried out with “flux conserving” equilibrium calculations in which the total rotational transform profile was prescribed. Plasma current is a free variable which can not be controlled. Optimization of QA inevitably leads to configurations whose external rotational transform is smaller than that of the fixed-boundary equilibrium that the coil is designed to mimic.

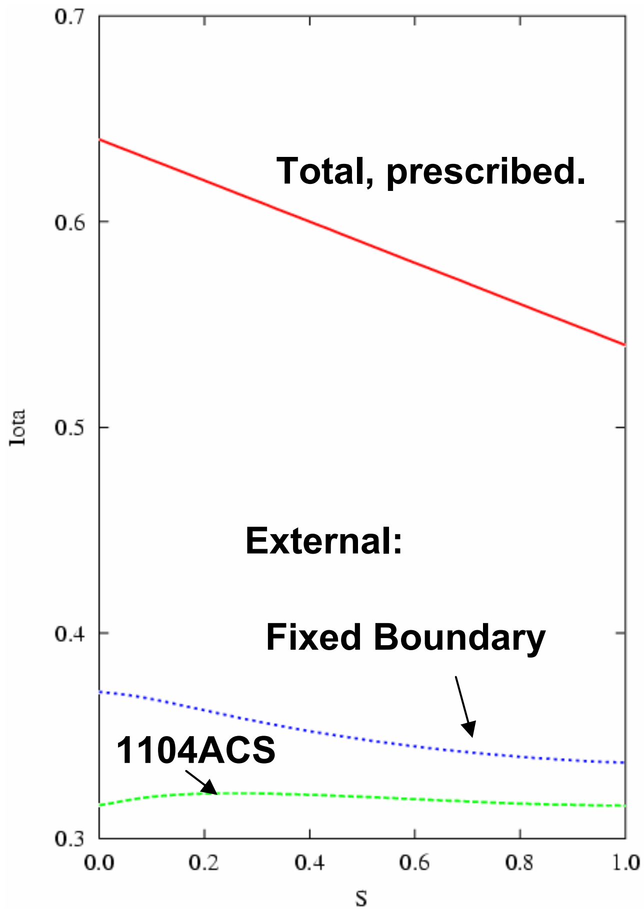

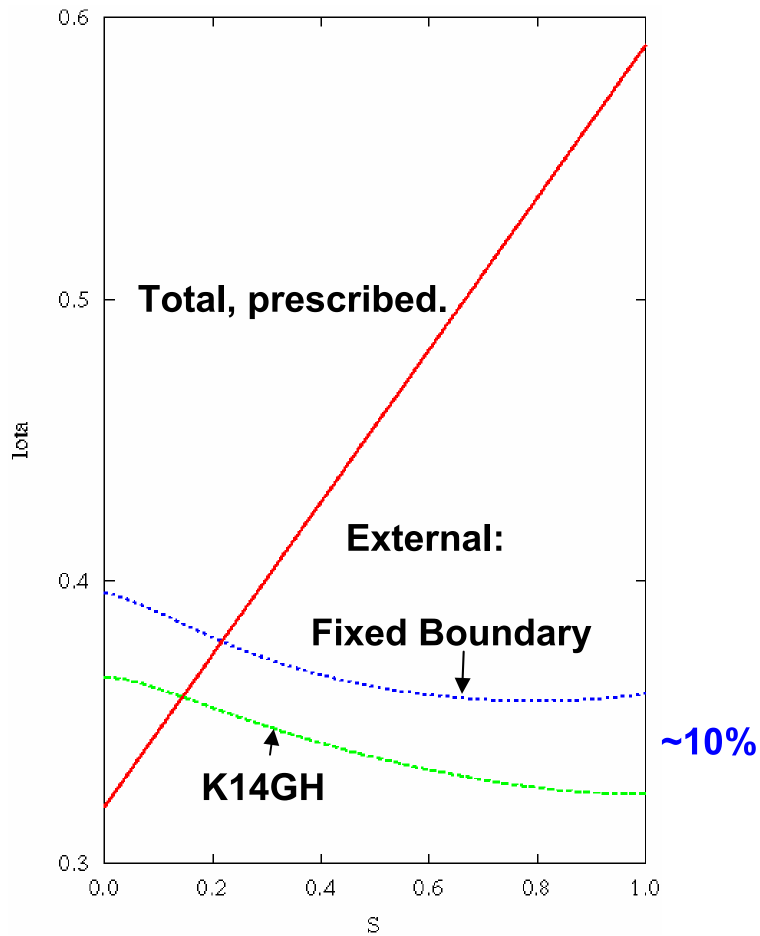

Rotational transform versus normalized toroidal flux.

A coil design with very low α loss (external transform constraint not imposed)

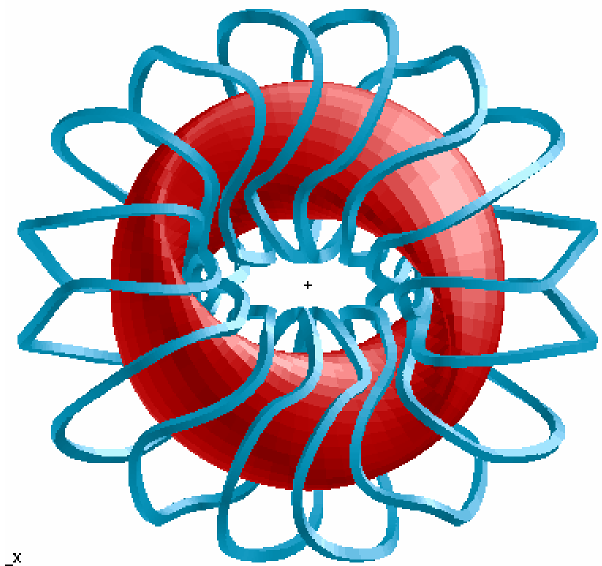

Modular Coils for MHH2-K14: K14JD

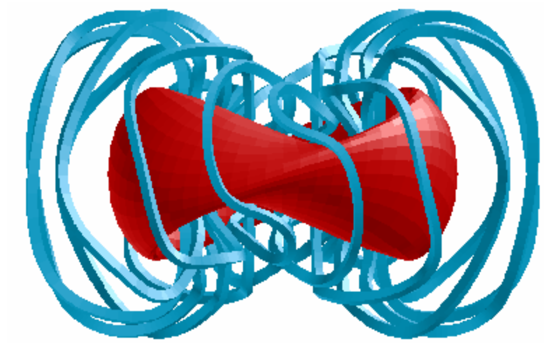

No. of Coils: 8/period

Different Types of Coils: 4

R/Δ_{min} (coil-plasma)=5.5

R/Δ_{min} (coil-coil)=12.6

I /R-B (max)=0.32 MA/m-T

B(max)/B(0) = 2.0 for 0.4 m x 0.4 m conductor

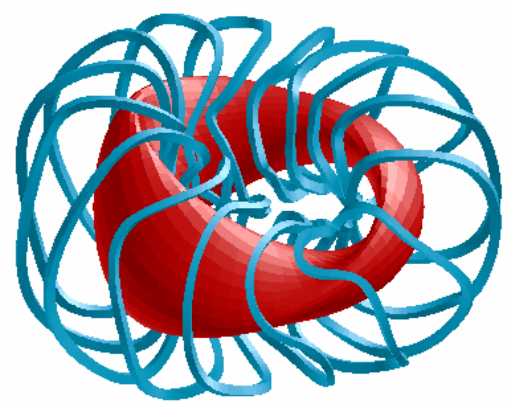

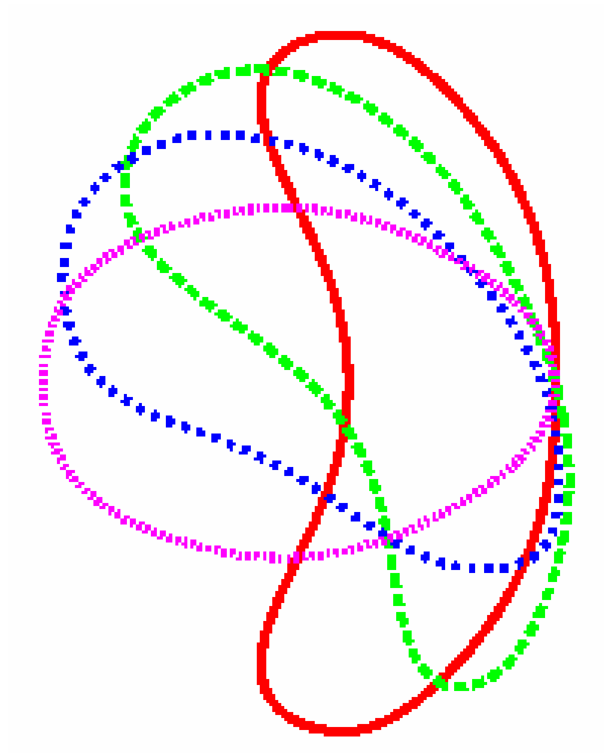

LCMS of the free-boundary equilibrium constructed from K14JD using VMEC.

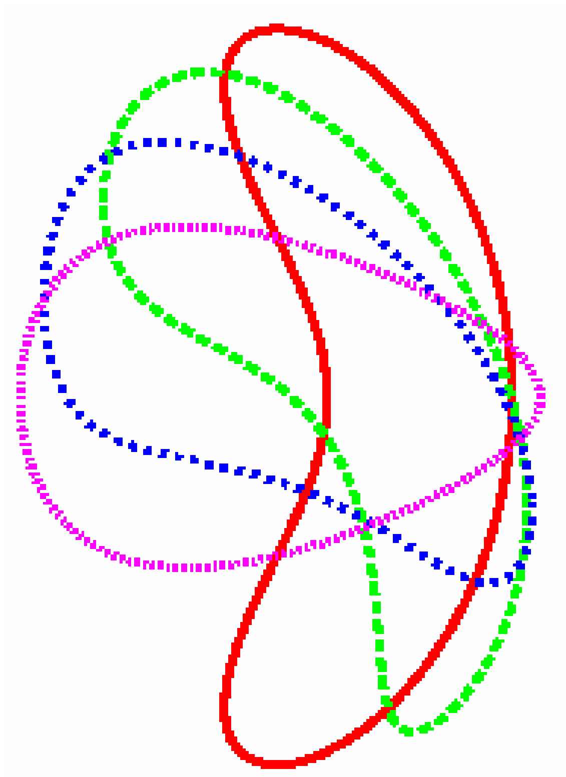

LCMS of the MHH2-K14 fixed-boundary equilibrium.

Comparison of residues in magnetic spectrum: reconstructed with K14JD versus the original, showing that the free-boundary equilibrium has superior QA and excellent confinement for α particles.

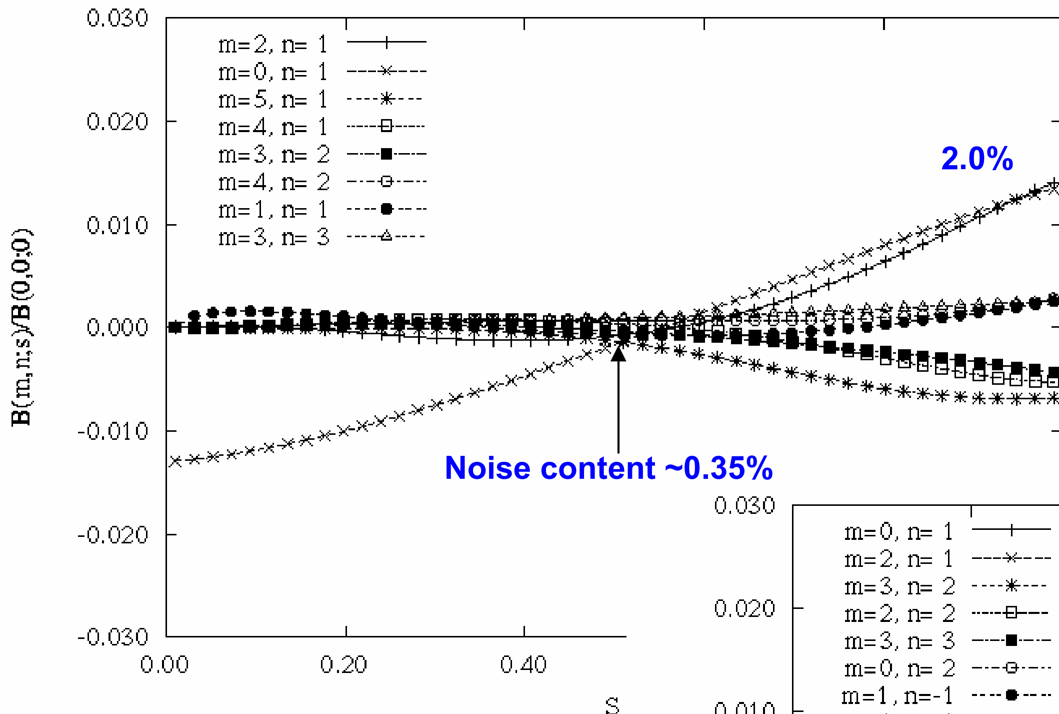

Free–boundary plasma, K14JD coils:

Effective ripple <0.73%

α energy loss in model calculation < 2%

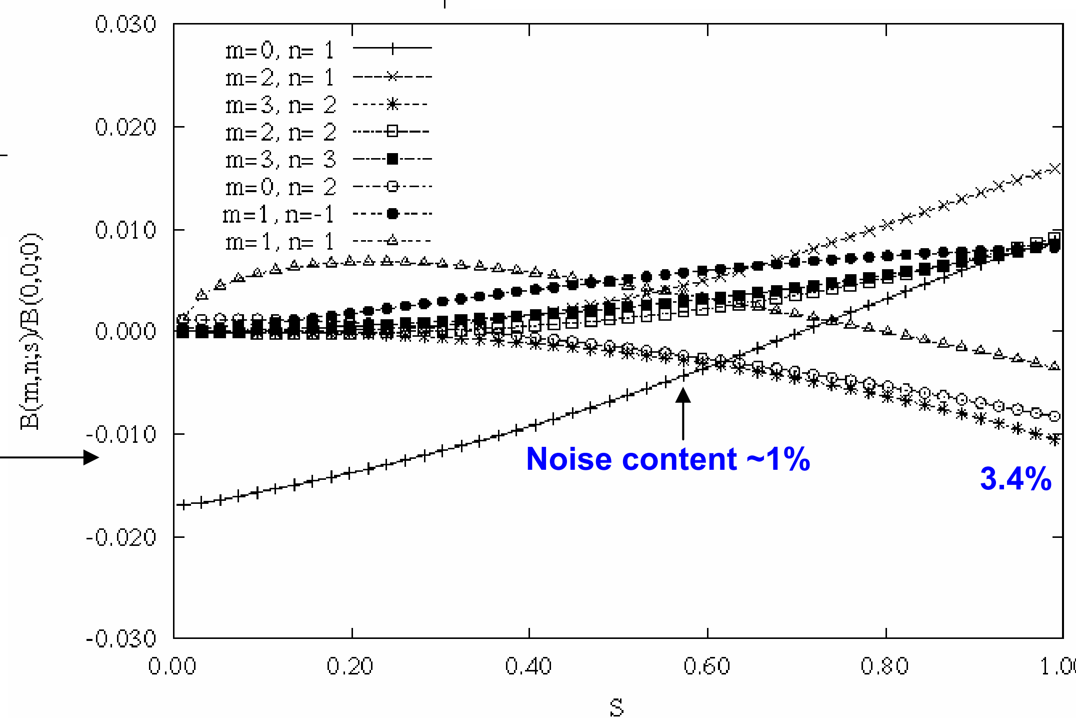

Fixed –boundary plasma:

Effective ripple <0.78%

α energy loss in model calculation ~6.5%

Magnetic field strengths plotted along several segments of field lines indicate that there are few secondary ripple wells, particularly in regions near r/a~0.7 where the residue is the lowest.

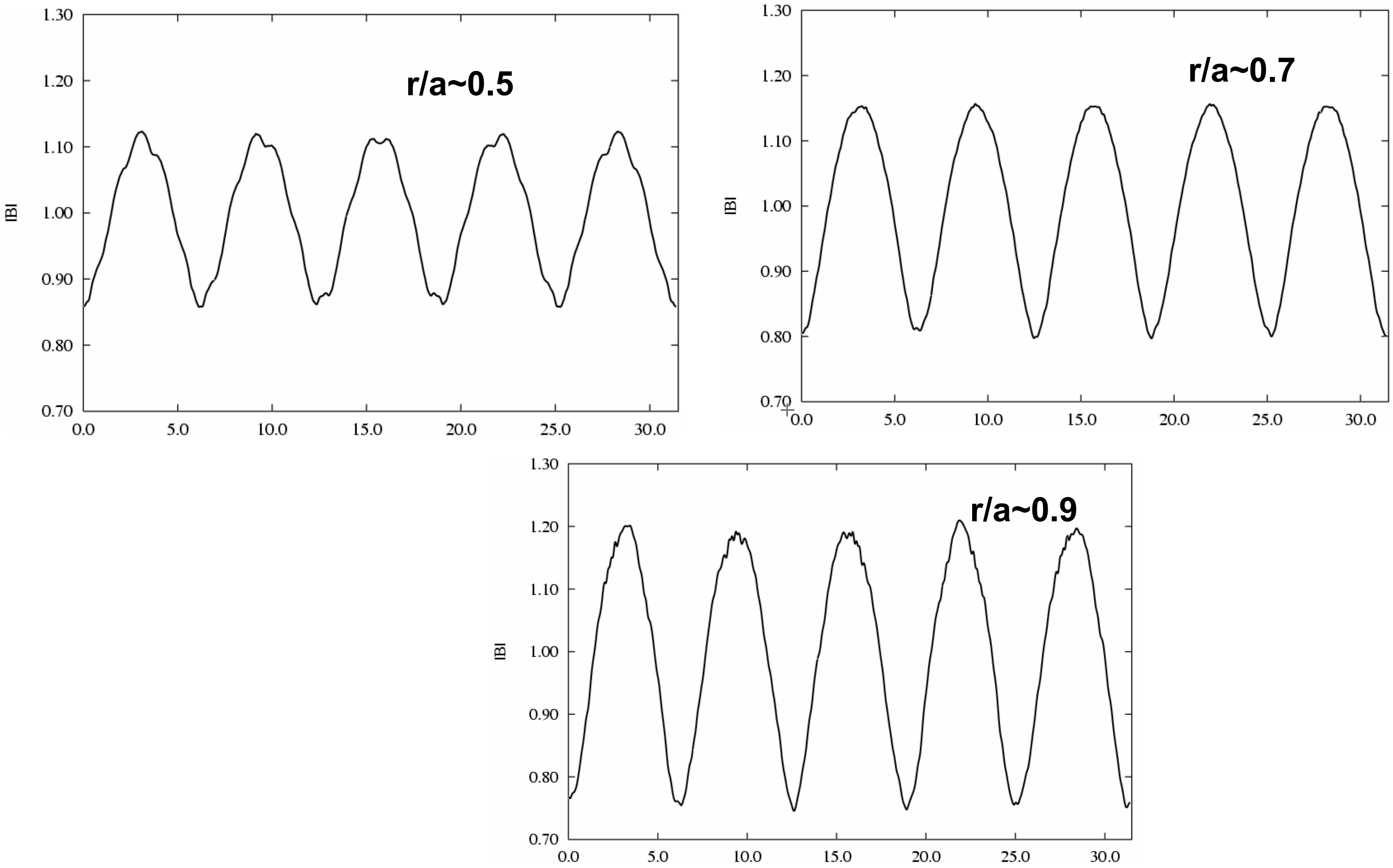

|B| versus poloidal angle θ in radians along field lines starting @ φ=0, θ=0.

Comparison of rotational transforms, reconstructed with K14JD versus the original fixed-boundary plasma, showing that the external transform in the free-boundary equilibrium is significantly lower.

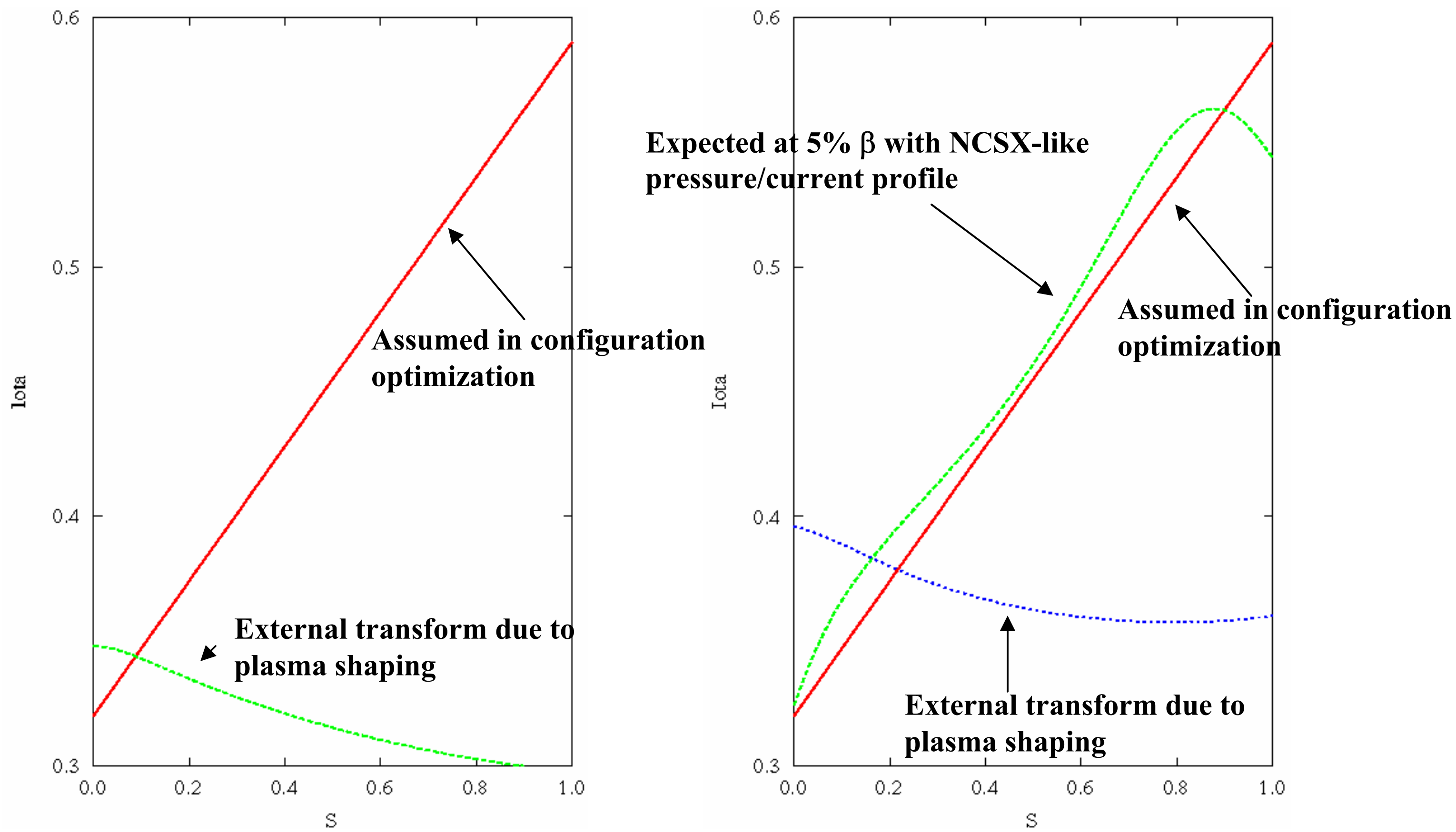

Rotational transform versus normalized toroidal flux. Left frame: free-boundary equilibrium due to K14JD. Right frame: fixed-boundary equilibrium.

A coil design with the prescribed plasma current density (constraining total rotational transform)

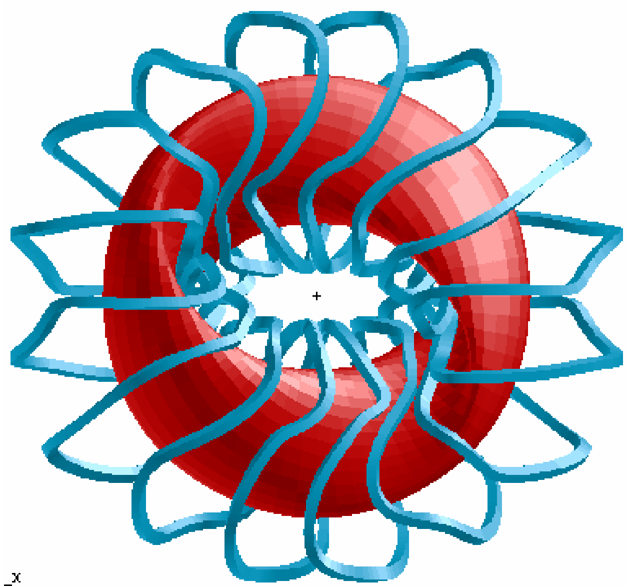

Modular Coils for MHH2-K14: K14LA

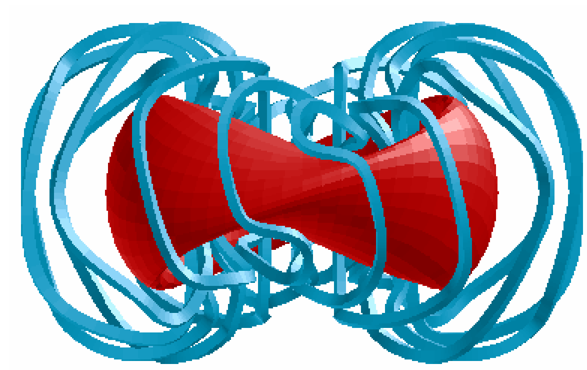

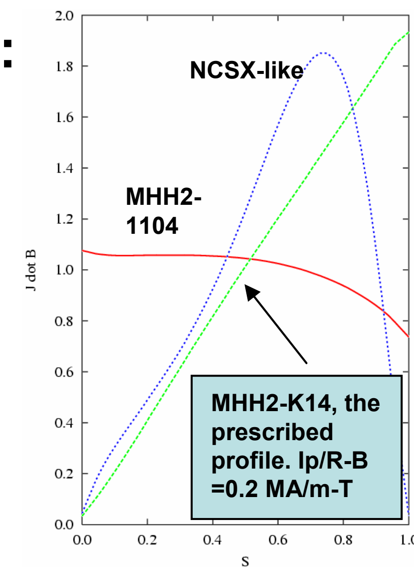

No. of Coils: 8/period

Different Types of Coils: 4

R/Δ_{min} (coil-plasma)=5.5

R/Δ_{min} (coil-coil)=10.3

I /R-B (max)=0.32 MA/m-T

B(max)/B(0) = 1.9 for 0.4 m x 0.4 m conductor

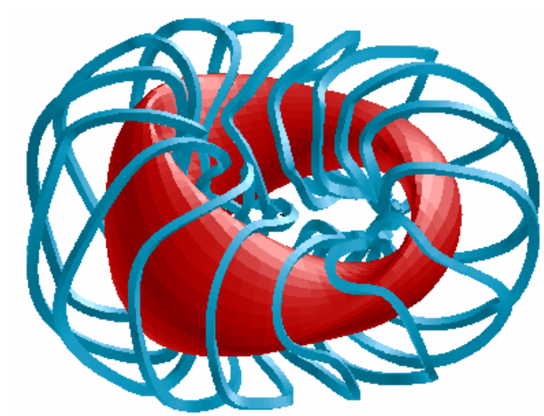

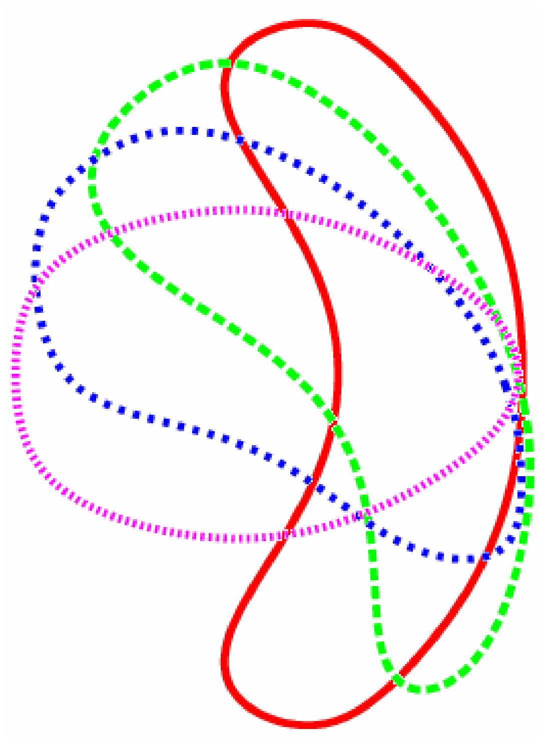

LCMS of the free-boundary equilibrium constructed from K14LD using VMEC with m=7, n=8.

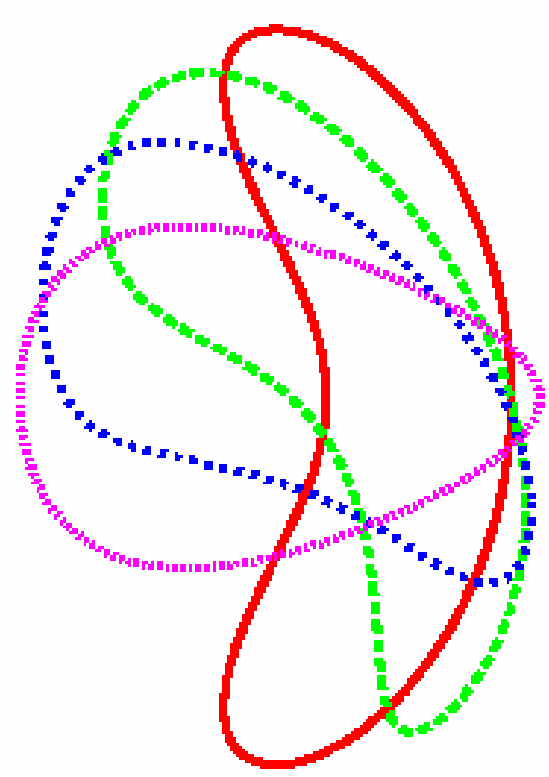

LCMS of the MHH2-K14 fixed-boundary equilibrium.

Comparison of rotational transforms, reconstructed with K14LA versus the original fixed-boundary MHH2-K14, showing both internal and external transforms are mostly recovered in the free-boundary equilibrium.

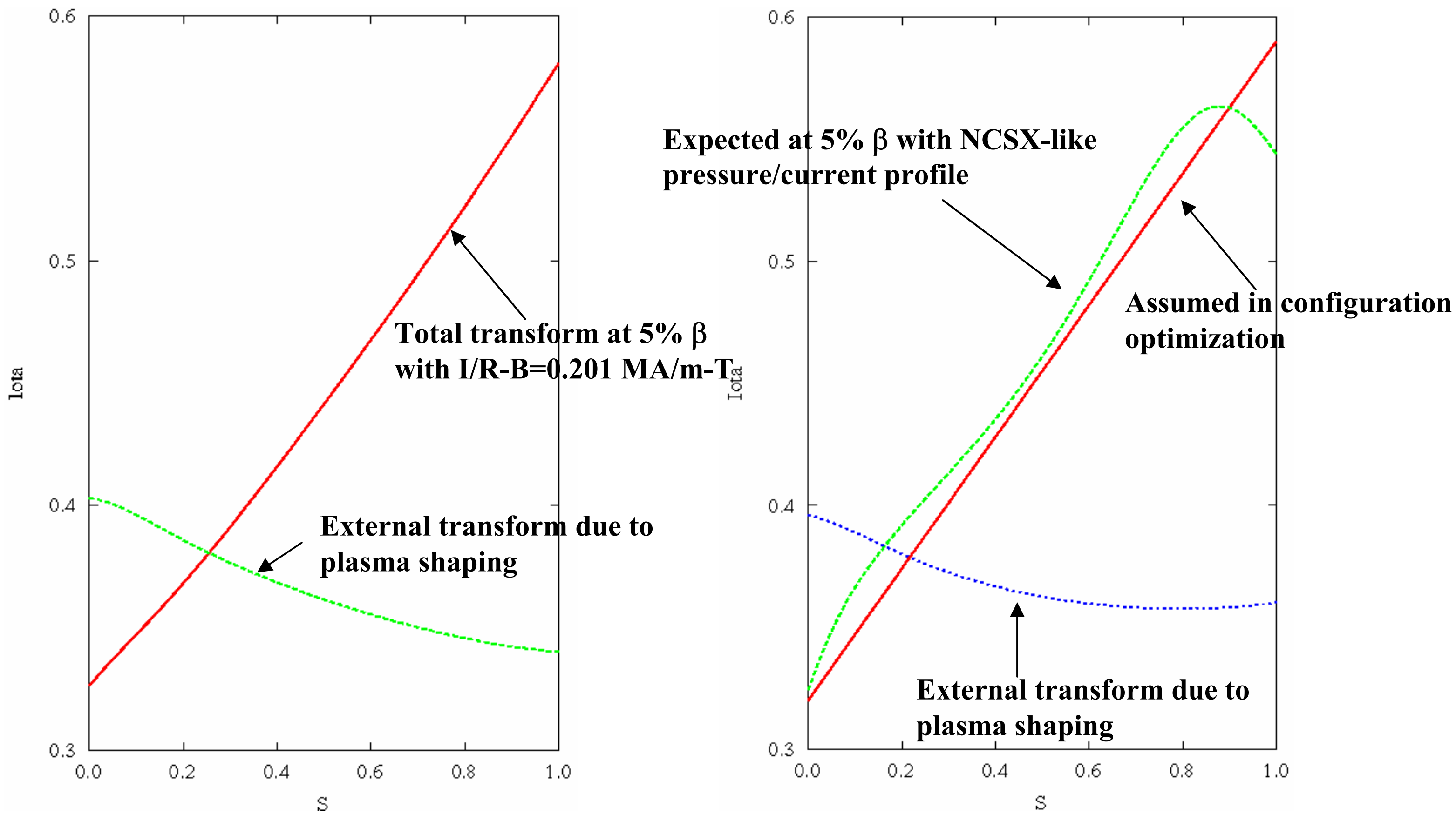

Rotational transform versus normalized toroidal flux. Left frame: free-boundary equilibrium due to K14LA. Right frame: fixed-boundary equilibrium.

Comparison of residues in magnetic spectrum: reconstructed with K14LD versus the original, showing that K14LD has significantly better QA.

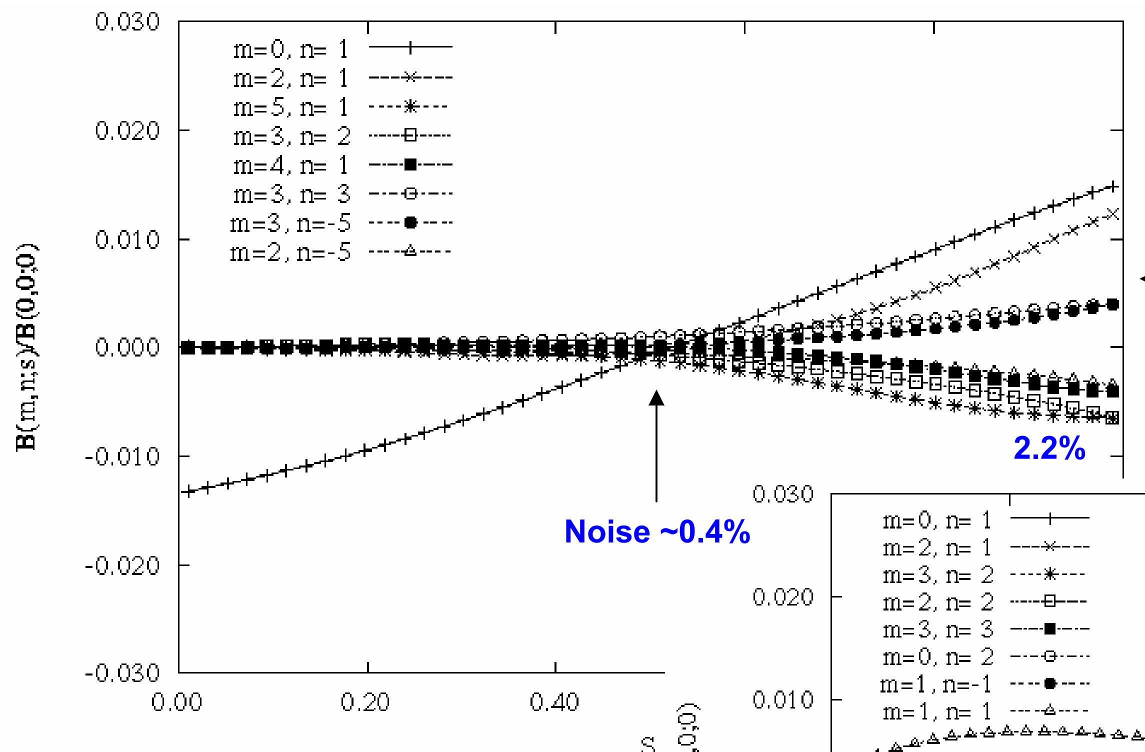

Free–boundary plasma, K14LA coils:

Effective ripple <0.8%

α energy loss in model calculation < 5%

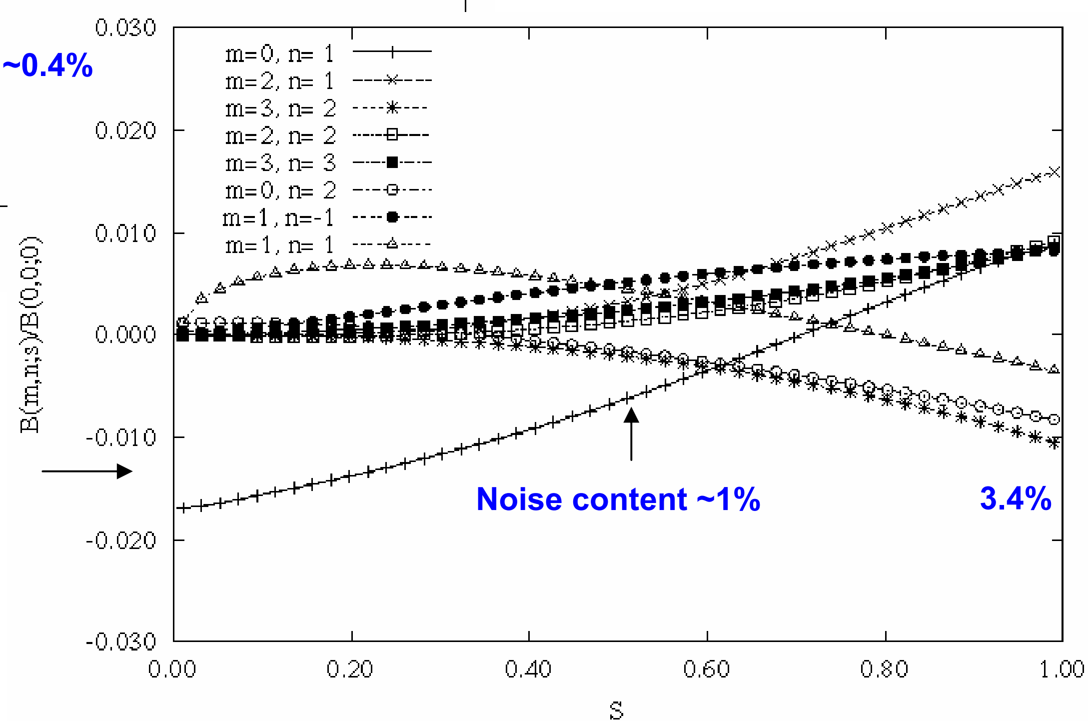

Fixed –boundary plasma:

Effective ripple <0.8%

α energy loss in model calculation ~6.5%

Magnetic field strengths plotted along several segments of field lines indicate that there are few secondary ripple wells for r/a<0.7. Secondary ripples are mostly on the high field side of the configuration.

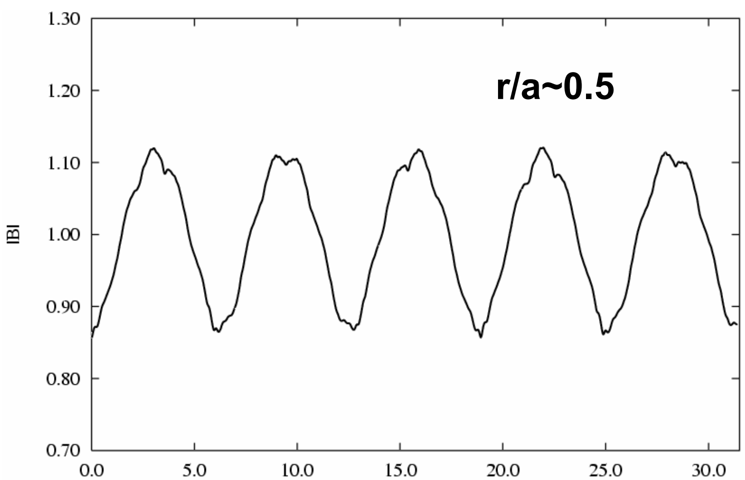

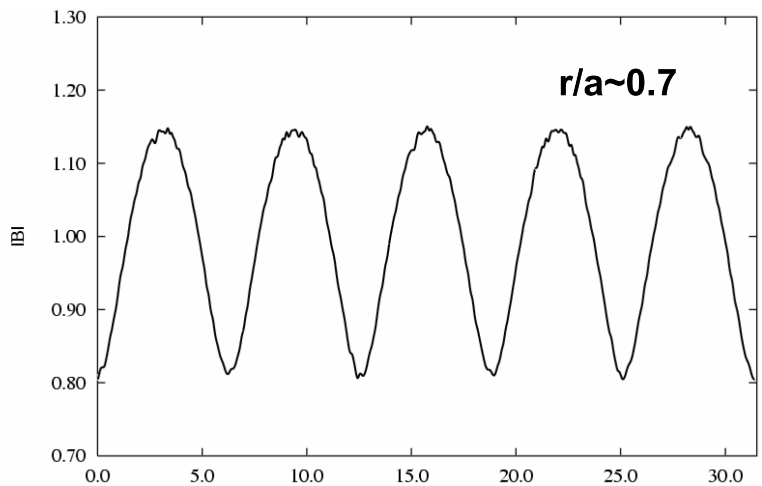

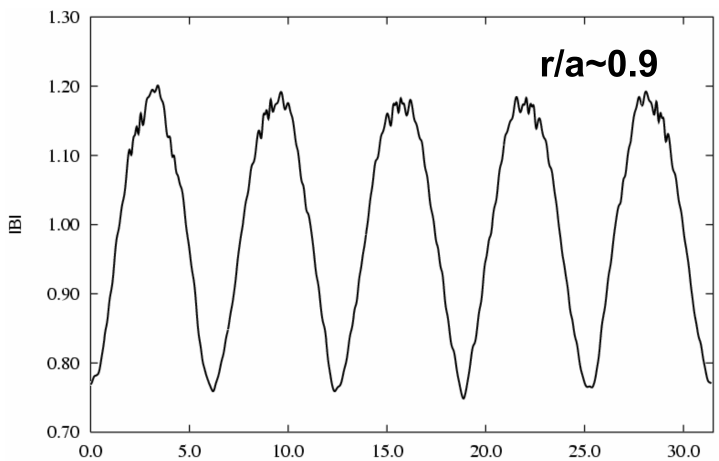

|B| versus poloidal angle θ in radians along field lines starting @ φ=0, θ=0.

KJC167

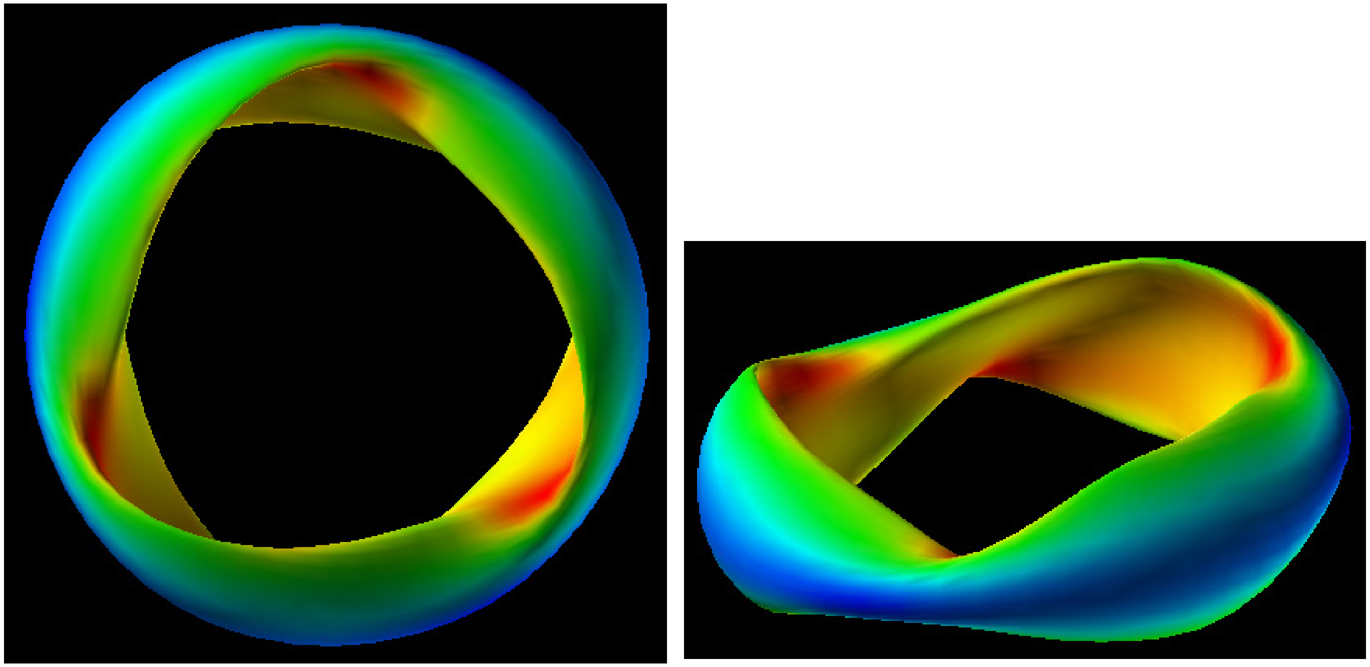

Plane and perspective views of last LCMS geometry and |B| in real space.

KJC167 is a 3 field-period, aspect ratio 6 configuration of the SNS/LPS family in which the iota profile is selected to minimize the impact of low order resonance on the flux surface integrity. In this case, the external iota has a strong negative shear, but the iota at operating β is expected to have a small but positive shear in most of the plasma volume.

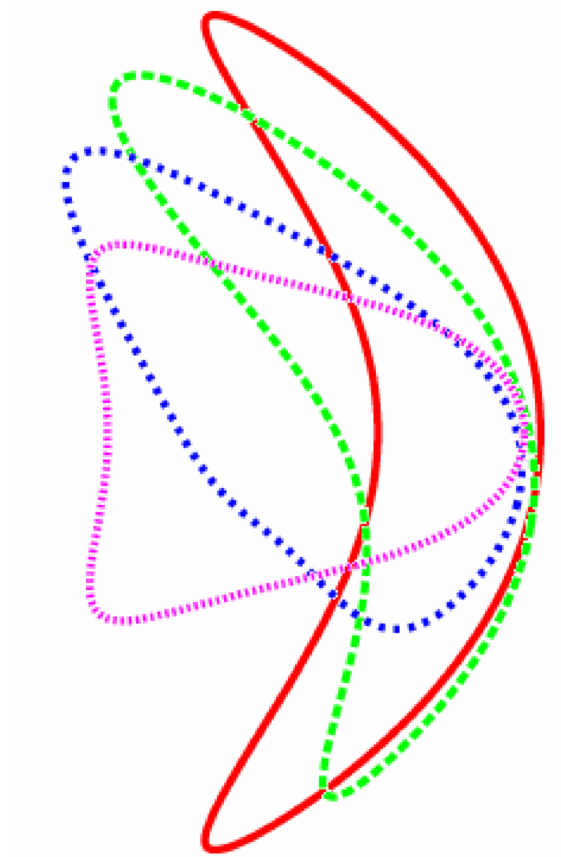

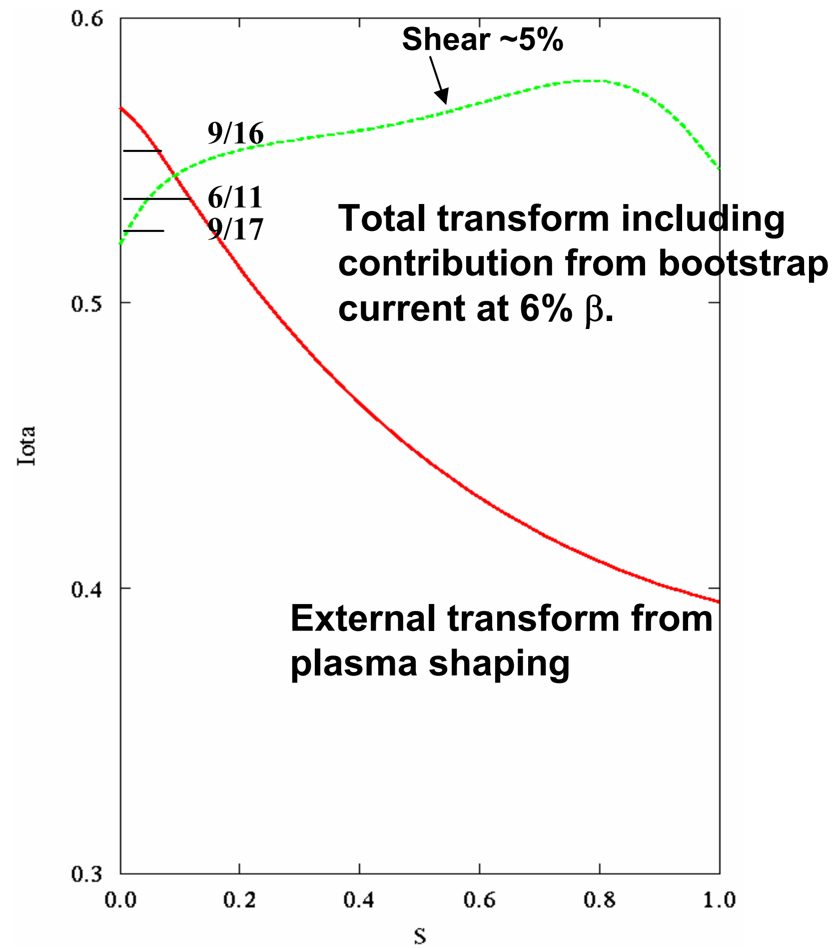

Minimizing non-axisymmetric residues and effective ripples resulted in good quasi-axisymmetry in KJC167. The effective ripple @s=1 is 0.35% at 6% β and the overall "noise" is <2.5%.

|B| on last LCMS in U-V space

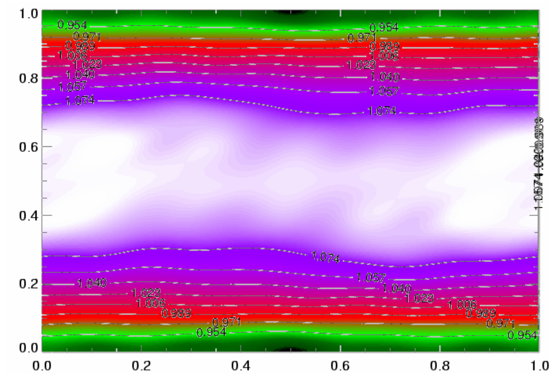

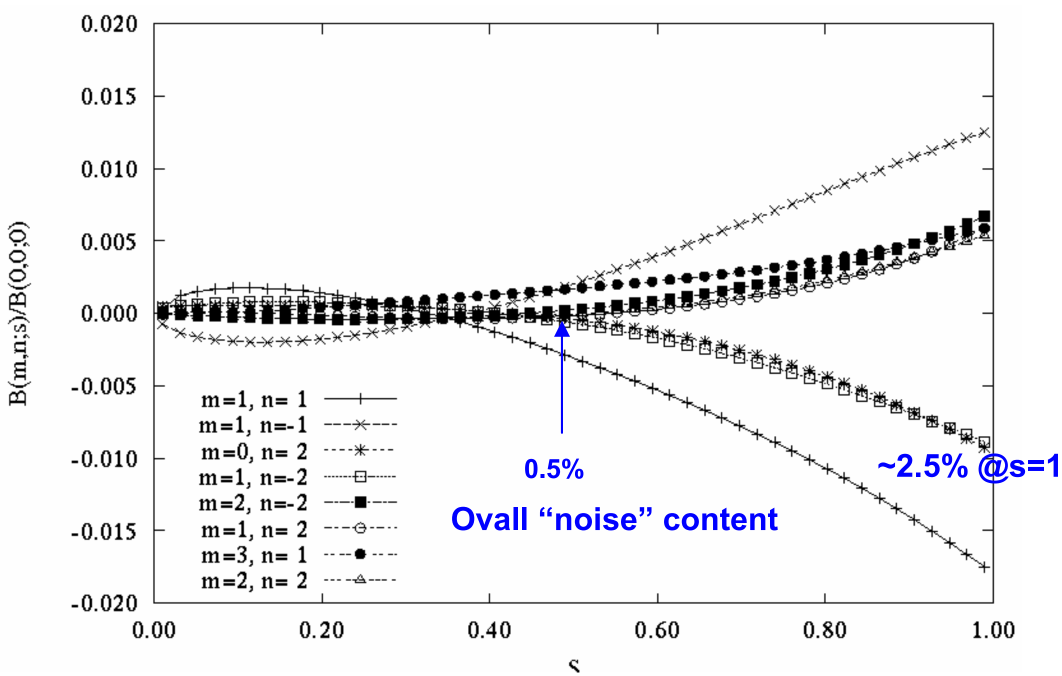

Eight major non-symmetric components in the magnetic spectrum plotted as function of normalized toroidal flux.

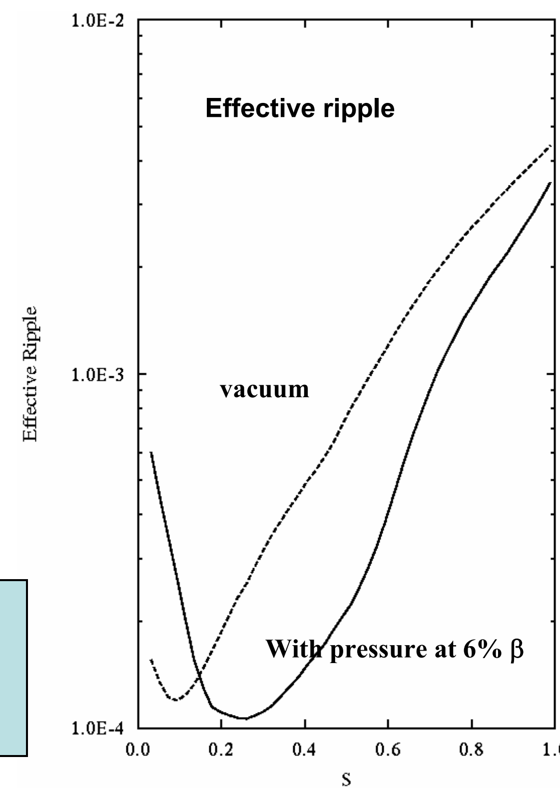

$$B = \sum B_{mn} \cos(m\theta - [n - \iota m]\varphi)$$

$$\text{noise} = \sqrt{\frac{\text{magnetic energy, nonsymmetric components}}{\text{magnetic energy, symmetric components}}}$$

LPK_061405

Loss of α energy is ~8% in one slowing down time in our model calculation.

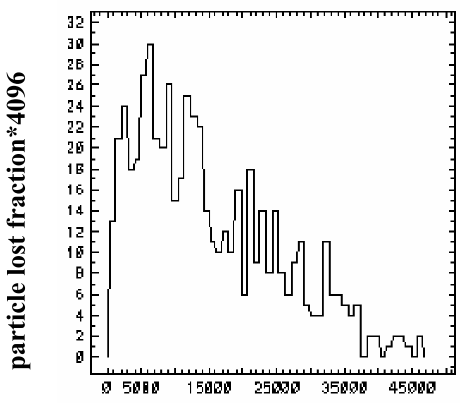

Transit time (in units of 6.38 μs)

Particle loss as function of time.

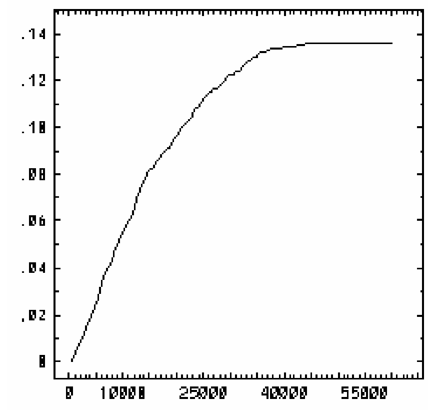

Transit time (in units of 6.38 μs)

Cumulative particle loss.

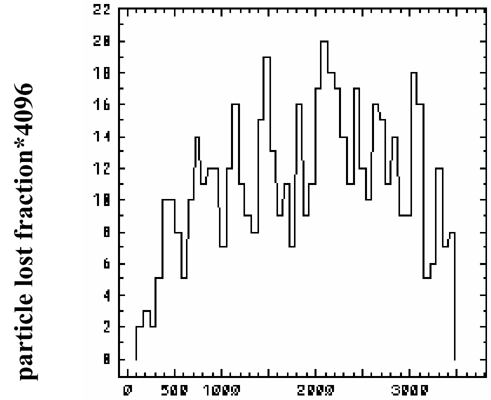

Energy (keV)

Energy loss distribution

Scatter diagram showing distribution of lost particles in energy, toroidal and poloidal angular space on LCMS.

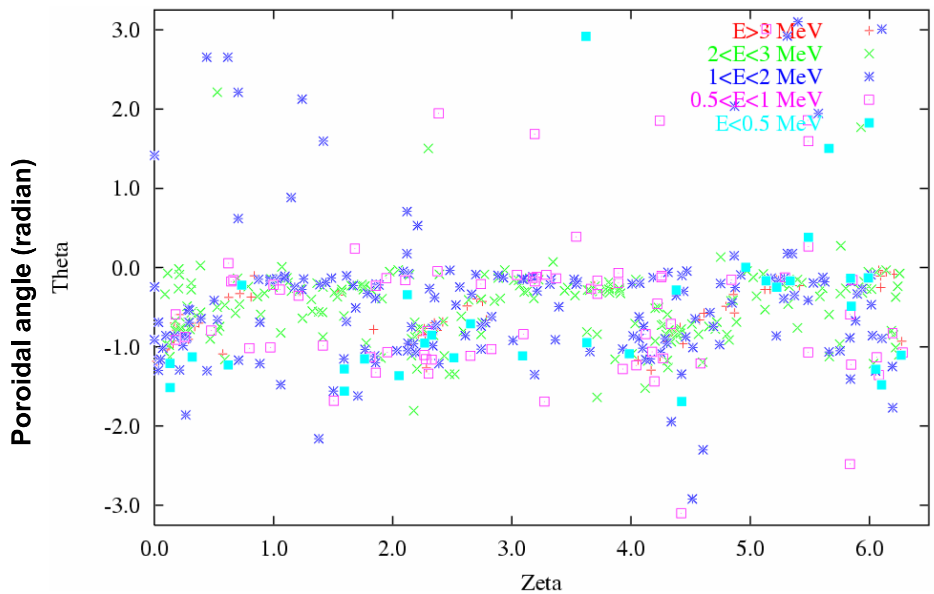

Toroidal angle (radian)

Excellent quality of flux surfaces is observed in most of the plasma for KJC167 at 6% β as seen below based on a PIES calculation.

Equilibrium calculated by PIES @6% β.

Poincaré plot in r-θ at φ=0.

In Cartesian

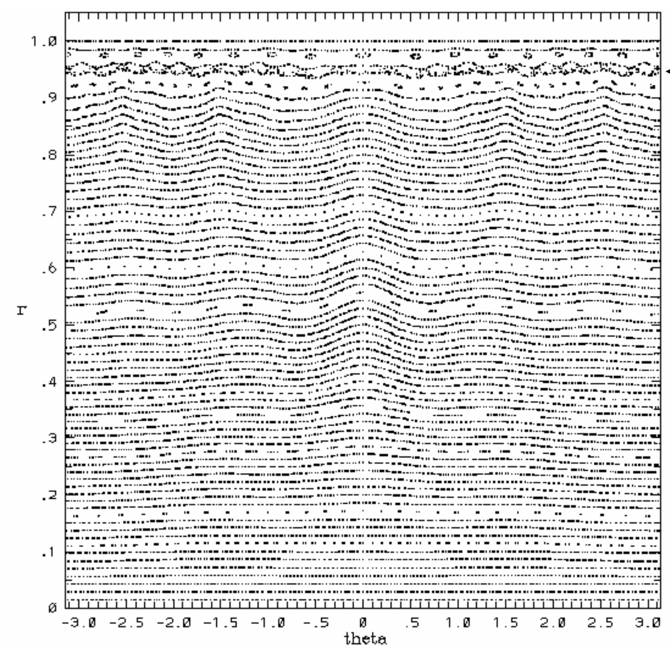

m=16

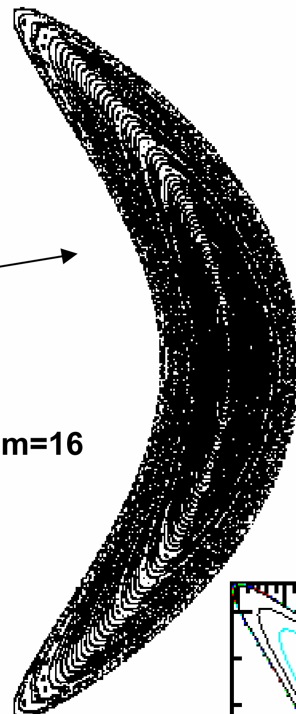

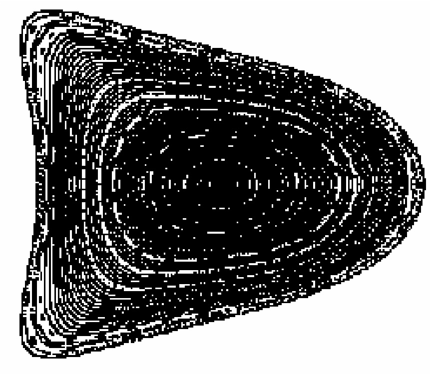

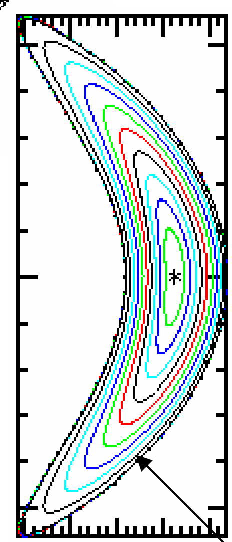

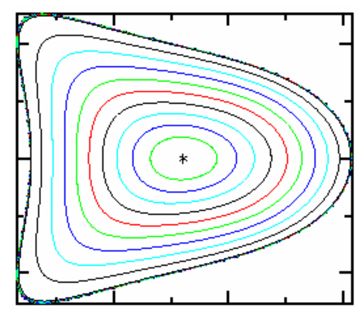

PIES and VMEC solutions are consistent.

Equilibrium calculated by VMEC

KJC167 is stable to the m=1, n=0 vertical mode according to the Terpsichore calculation (no feedback control necessary) and is slightly unstable to both low and high-n internal modes at β=4%.

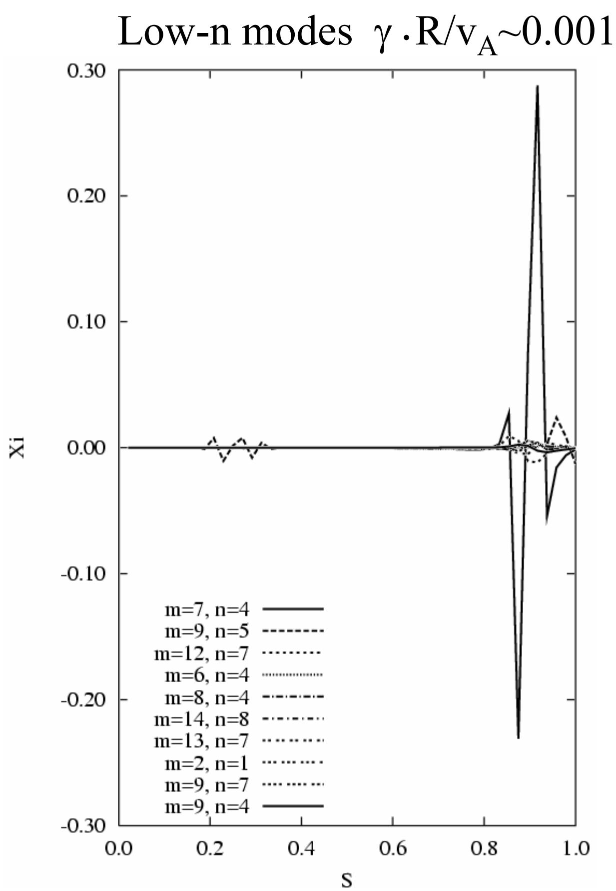

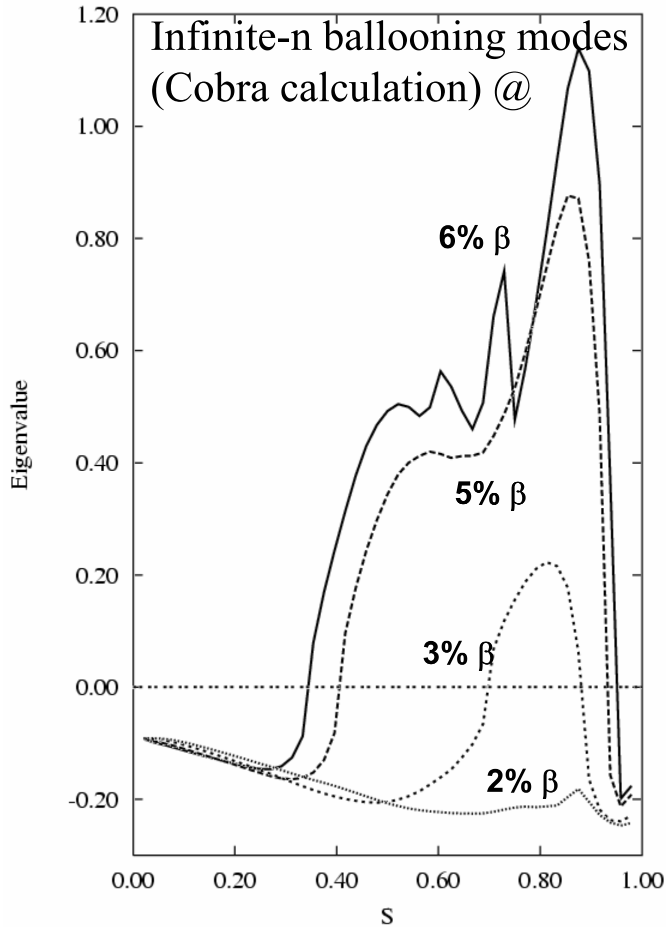

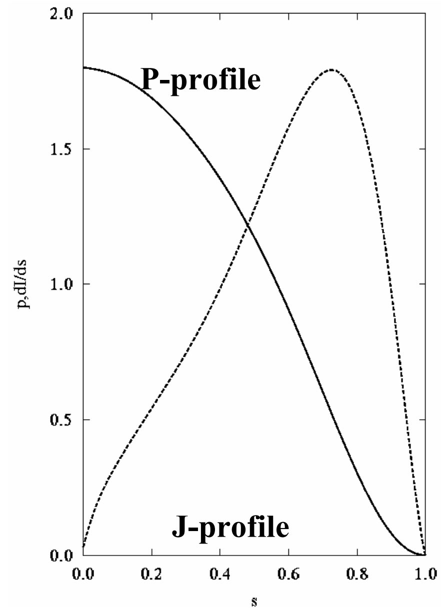

Note: stability analyses were based on the pressure and current profiles given above. Profiles may be further optimized to improve MHD stabilities to both the local and global modes.

KJC167 may be unstable to free-boundary modes for β~6% according to the Terpsichore calculation primarily due to the m=2, n=1 mode, but it could be made stable with more flux surface shaping to improve the local shear. It may also be made more stable by choosing more optimized pressure and current profiles.

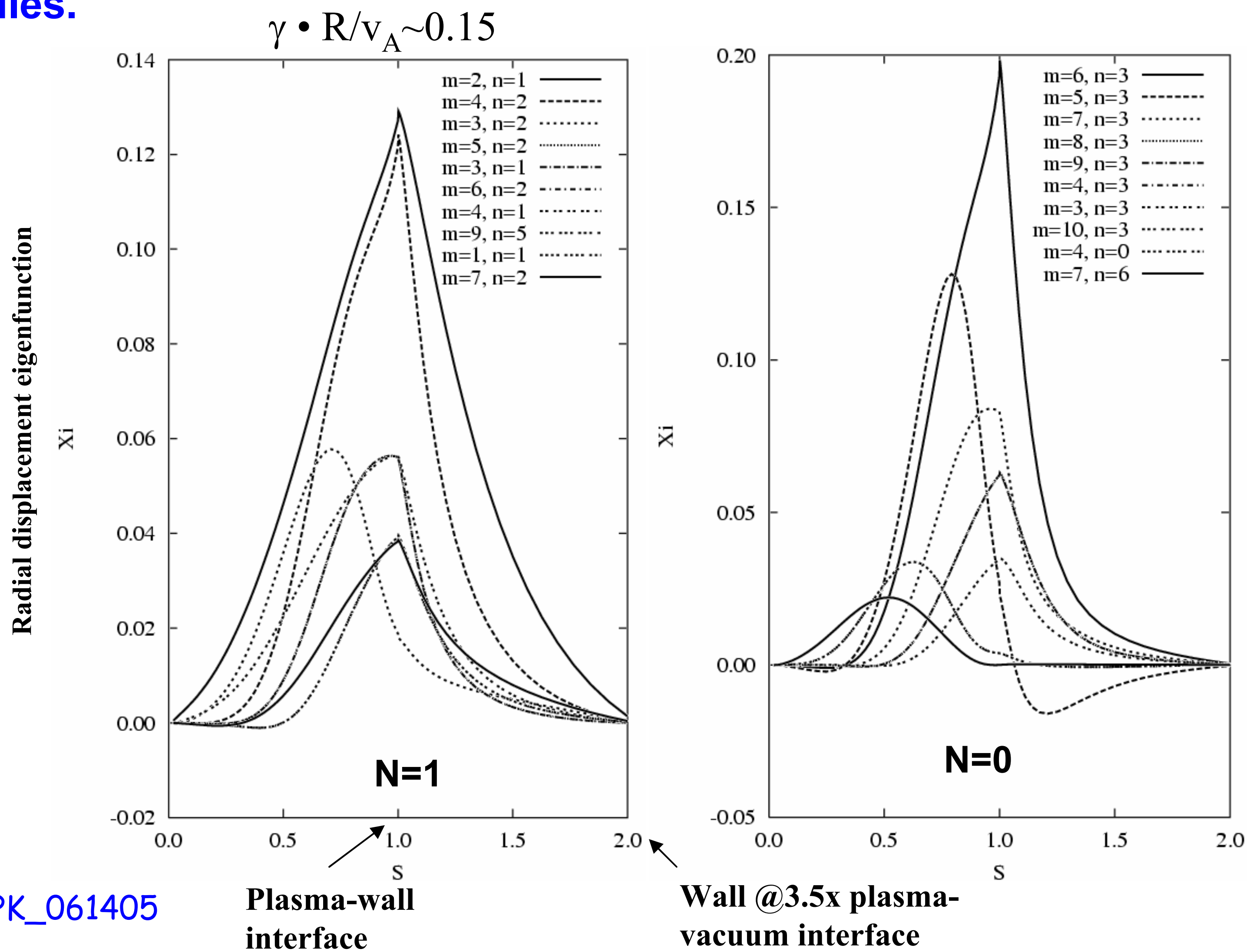

These modes may be stabilized by further shaping.

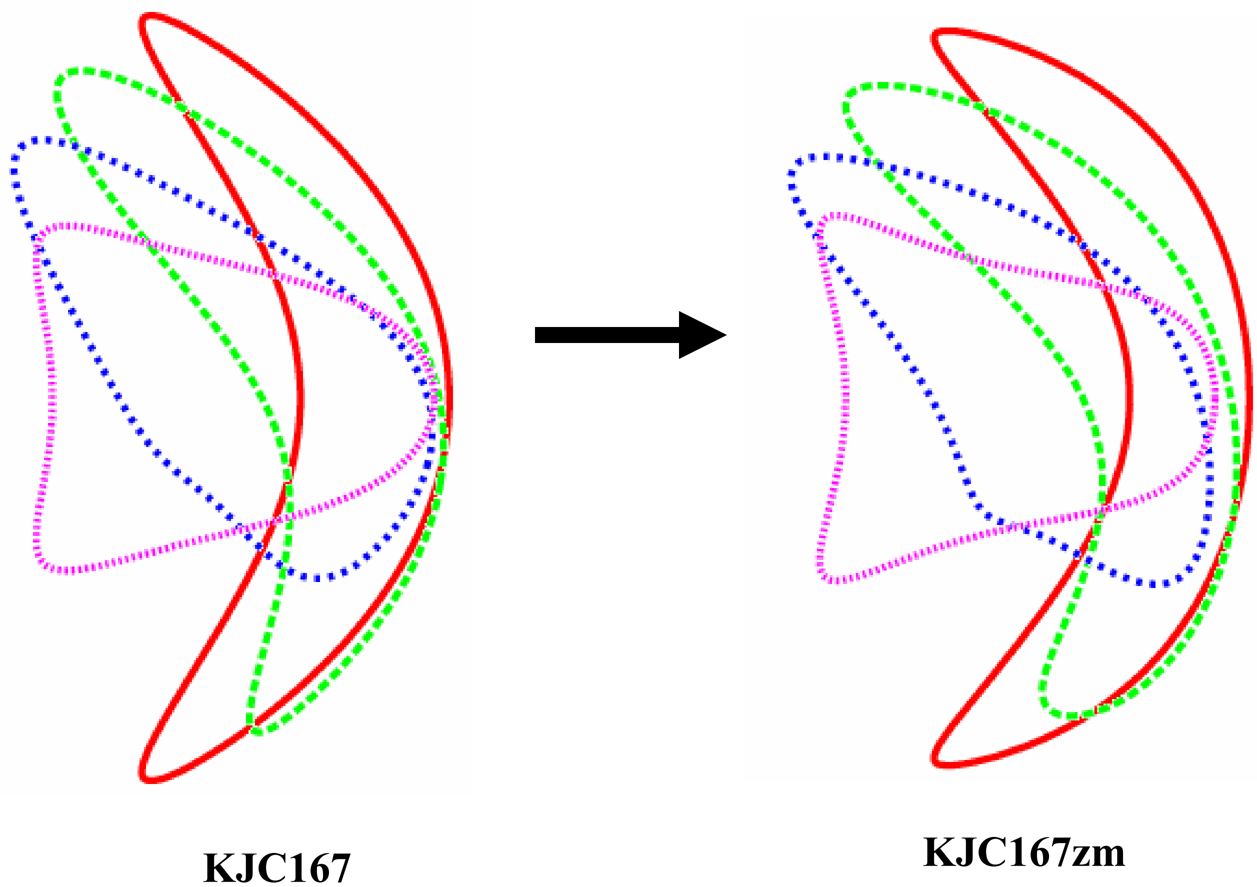

Ballooning modes may be simultaneously improved with the additional shaping to improve the stability to the external kinks.

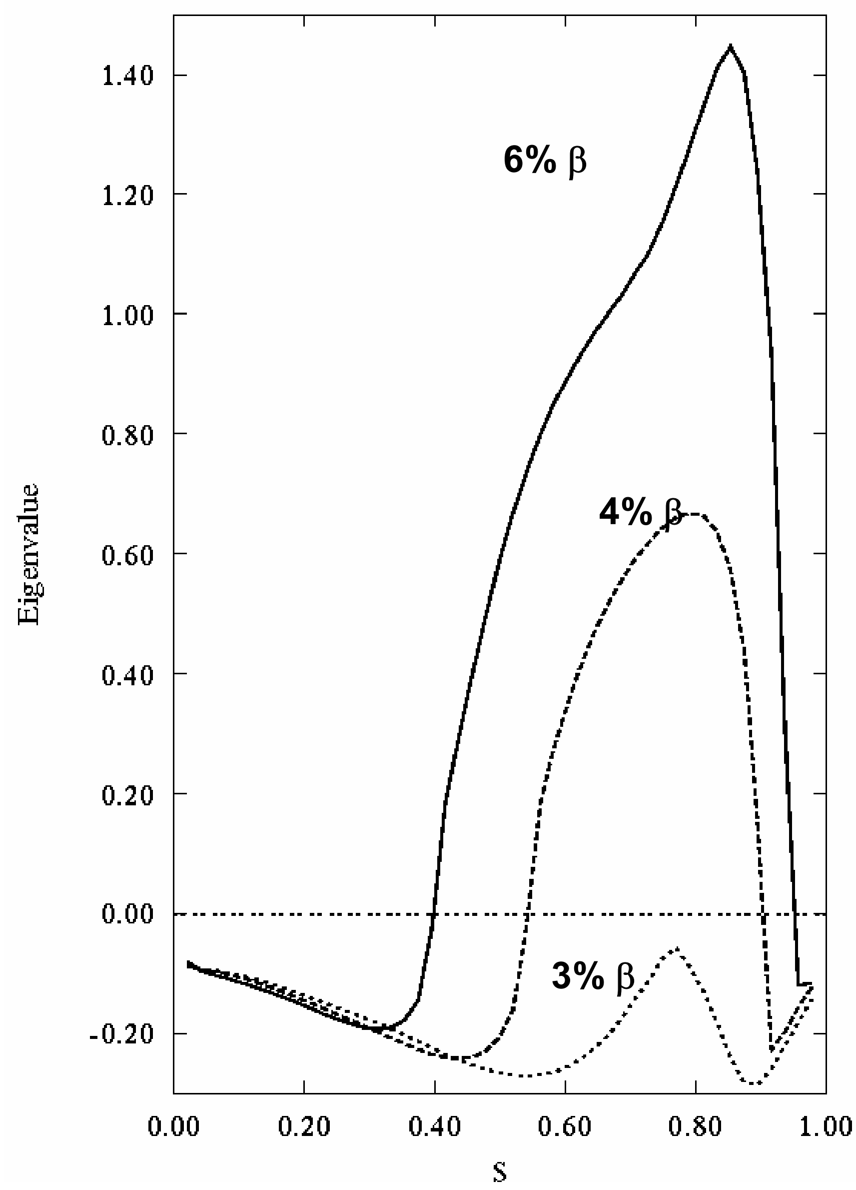

But, effective ripples are increased by more than 60% for r/a>0.8 in the kink stabilized configuration, resulting in enhanced loss of α particles. The ε_{eff} is still small, less than 0.6%, however.

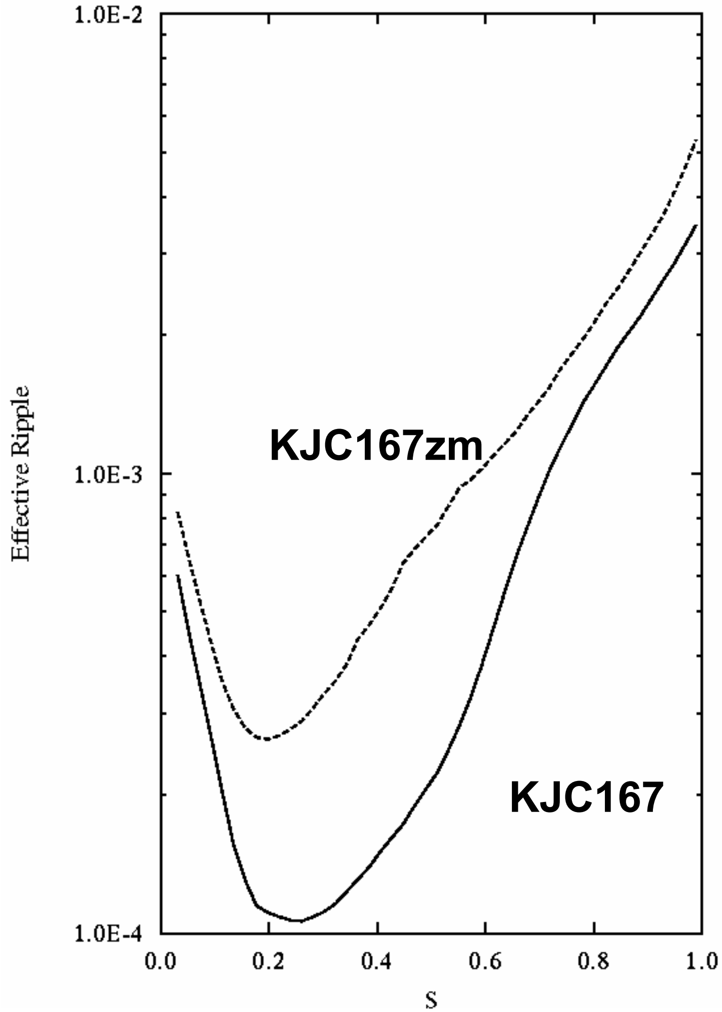

A proposed design for the modular coils is to have 6 coils/period with coil aspect ratio R/Δ_{min}(C-P)~6. The example given here, KJC167-M05, based on equal coil currents, has smooth contours with small toroidal excursion.

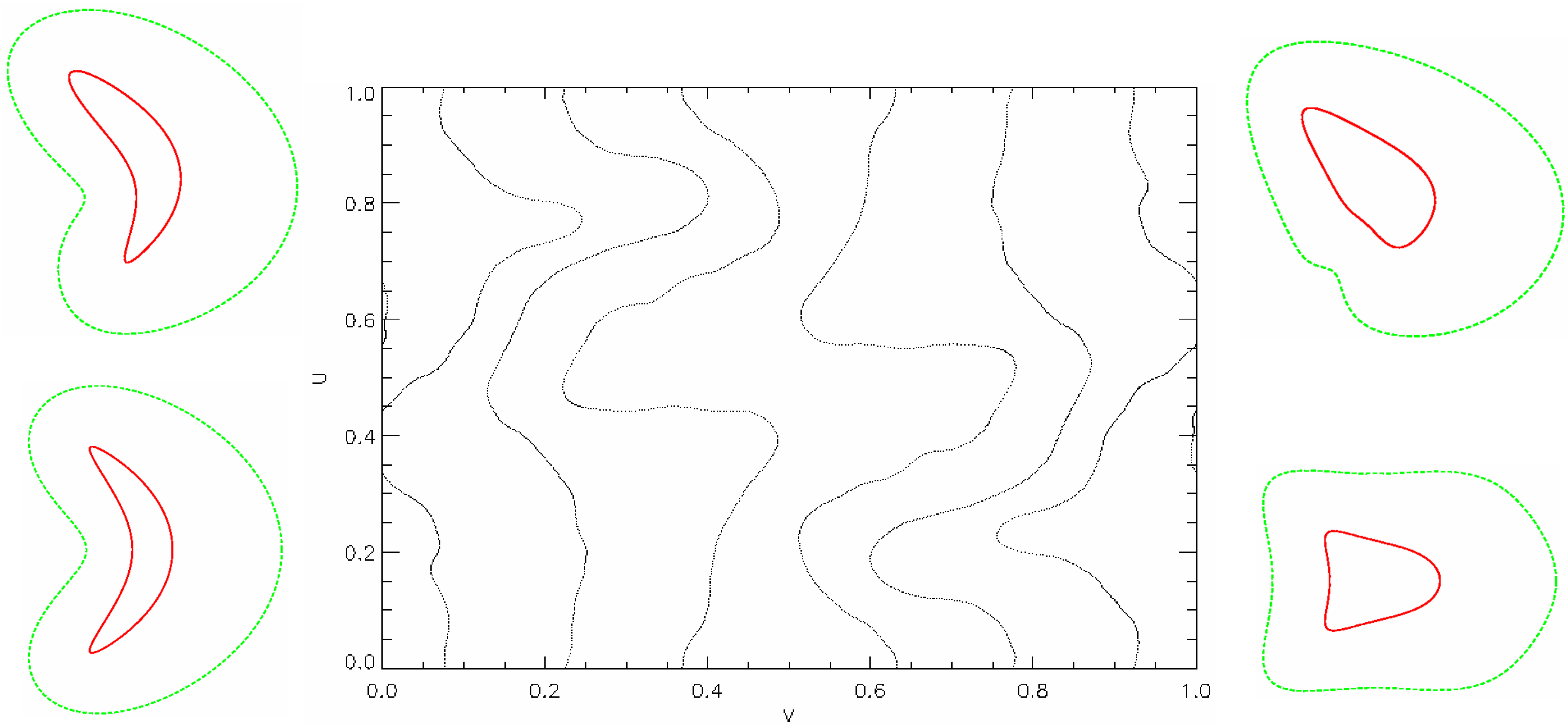

Coil contours viewed on "U-V" plane of the winding surface in one field period.

Comparison of KJC167-M05 and NCSX-M50 showing that the complexity of the two designs is of the same level.

KJC167-M05

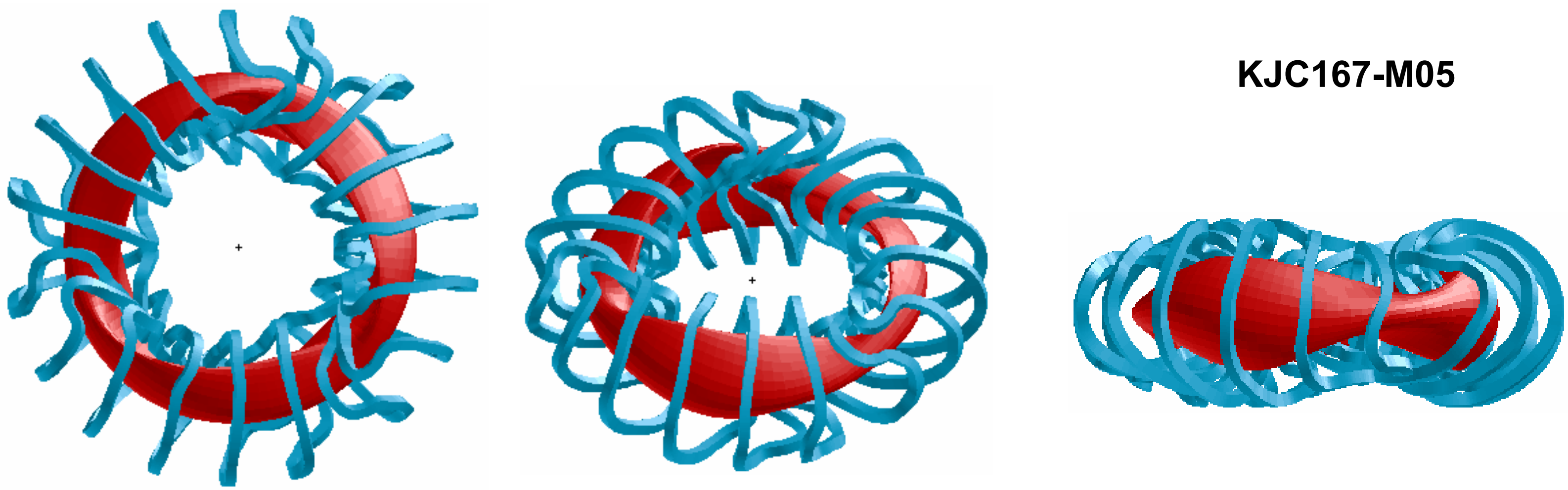

NCSX-M50

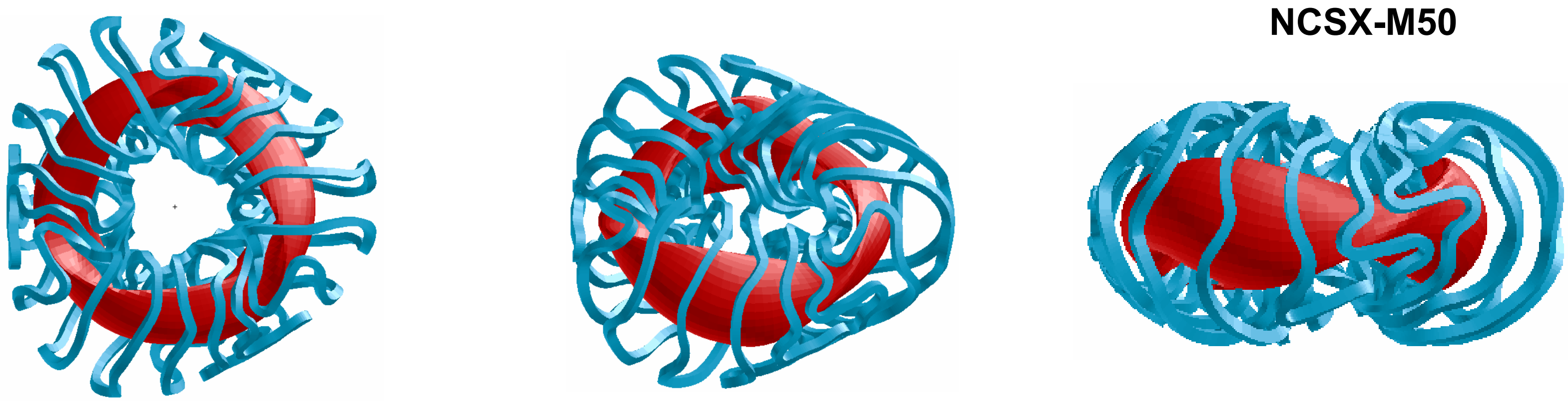

Summary of coil properties based on a design which tried to minimized the normal field residues on the last closed magnetic surface of the fixed-boundary plasma KJC167.

KJC167-M05 Coil Characteristics:

No. of Coils: 6/period

Coils of Different Type: 3

B_n Error = 1.5 % (average), 5% (max)

R/Δ_{min} (coil-plasma)=6.0

R/Δ_{min} (coil-coil)=9.8

Winding surface area/R^2=21.0

I /R-B (max)=0.28 MA/m-T

coil lengths/R = 3.61, 3.55, 3.43

B(max)/B(0)=2.2 for 0.4 m x 0.4 m square conductor

Summary and Plans

- New modular coils are designed for MHH2 with 8 coil/period that have good engineering properties and superior quasi-axisymmetry in the free boundary equilibria with α energy loss typically < 10% in model calculations. These are achieved by directly targeting plasma and coil parameters important for reactor design considerations.

- We've also brought a 3 field-period, A=6 configuration, KJC167, to the same level of development as MHH2 and KQ26Q for the systems evaluation.

- We plan to re-examine NCSX-like configurations in the summer to seek ways of further improving the confinement of energetic particles and to optimize MHH2 coils to further push design limits. We also intend to seek ways to better integrate configuration design targets in the optimization process.